In comparison with most of the United States (U.S.), thunderstorm activity in the Pacific Northwest is relatively infrequent (Wallace, 1975; Changnon, 1988a and 1988b). The comparative lack of thunderstorm activity in this area owes primarily to its position east of the Pacific Ocean subtropical high pressure area. In the eastern U.S., located on the western side of the subtropical high, poleward moving air has undergone a long trajectory over tropical waters. In addition, systematic rising motions are generally found on the western sides of the subtropical anticyclones. In contrast, general subsidence tends to characterize motion on the eastern sides of these highs. This drier air, in sinking, is heated by compression and usually overlies a shallow humid marine layer. Hence, a more stable atmosphere frequently exists on the eastern sides of the subtropical highs (Palmen and Newton, 1969; Barnes and Newton, 1981).

Two essential ingredients are necessary for the formation of any thunderstorm, while a host of secondary factors may influence the type and intensity of the storms that do occur. The first necessary element is for sufficient moisture to exist, and the second is for adequate vertical motion to initiate precipitation. One of these factors without the other will likely preclude the formation of a thunderstorm. These primary factors are considered in a general context and also in terms of the Pacific Northwest region and its physical environment.

Sufficient moisture is necessary so that condensation can result from any lifting or turbulent mixing that takes place in the atmosphere. The moisture for most Pacific Northwest thunderstorms arrives primarily on westerly or southwesterly currents that are not part of the humid marine layer, but rather overlie it. This low-level moist layer tends to possess a fairly low wet-bulb potential temperature due to its passage over the cool California current and is prevented from much inland penetration by the coastal mountain ranges. The moisture content of the overlying Pacific air is fairly low, but lifting and/or heating during its passage over the western plateau increases the wet-bulb potential temperature in the lower atmosphere (1-2 km above ground level) to near that of maritime tropical air. The increase of the wet-bulb potential temperature near the surface, by itself or in combination with cooling aloft, results in destabilization of the air column (Palmen and Newton, 1969; Barnes and Newton, 1981).

Research has also shown that storms in the southern portion of this region receive a substantial amount of moisture from the tropical Pacific and Gulf of California (Hales, 1972; Hansen, 1975). This airflow is typically associated with the southwest monsoon regime which advects maritime tropical air into Arizona and adjacent states in the summertime, sometimes as far north as southern Idaho. This pattern has been well documented (Bryson, 1957a and 1957b; Sellers, 1964) to account for a substantial percentage of summertime rainfall in the southwest, mostly in the form of convective storms. The southwest monsoon pattern also brings in air from the Gulf of Mexico, when the summertime Bermuda High is located west of its normal position. Moisture from the Gulf of Mexico was found to occur almost exclusively at upper levels of the atmosphere (700 to 300 mb), rather

than at low levels (below 700 mb) in a study by Reyes and Cadet (1988). Several very recent studies (Carleton et al., 1990; Hagemeyer, 1991) have also stressed the predominance of Gulf of California moisture, rather than Gulf of Mexico, in producing warm season precipitation in the west and southwest United States.

A second requisite factor for the development of convective rainfall is adequate vertical motion. Upward vertical motions in the atmosphere can occur under a wide variety of spatial and temporal scales. These range from large-scale synoptic areas ahead of long-wave troughs, frontal areas, mesoscale convergence zones down to localized thermals. The development of sufficient vertical motion relies on a number of critical factors. According to McNulty (1983), these factors include unstable air or a destabilizing influence, divergence aloft and low-level convergence. Lifting may also be caused by other factors including orography, terrain induced convergence, jet streaks, frontogenesis, positive vorticity and warm air advection, and convection due to the diurnal heating cycle.

Some large-scale meteorological patterns are more favorable for the development and maintenance of rising motions than others. At the synoptic scale, it is recognized that in the general region from an upper-level trough to the downstream ridge, there is upper-level divergence. In keeping with the law of mass continuity, there is in the lower levels general horizontal convergence with ascending motions that reach maximum values in the mid-troposphere. Such areas of large-scale ascending motions, while not generally sufficient to cause convection, can be said to "prepare the environment" for convection (Doswell, 1982). Strong upper-tropospheric divergence (above 500 mb) has also been found to be an important factor in generating the upward vertical velocities needed to support convective activity (Beebe and Bates, 1955; Bates, 1963).

The nature of convective storms depends greatly on the stability of the atmosphere in which they develop. The degree of thermodynamic instability plays a critical role on the strength of convection since it determines the capability of air to accelerate vertically. The potential of a column of air to attain the necessary thermal buoyancy for convection can be measured through a number of stability indices, a good review of which can be found in Peppler (1988). Destabilization of an initially stable air mass can occur over a period of hours, and be caused by various processes. Cooling aloft or the incursion of warm, saturated air near the ground are just two methods by which this may occur. This differential advection of various atmospheric properties in the vertical, results in net moistening at low levels and/or drying at upper levels (Doswell, 1982).

In the Pacific Northwest, it appears that direct surface heating usually plays the critical role in destabilizing the atmosphere to where convection can occur. Support for this contention lies in the seasonal and diurnal pattern of thunderstorm activity in the region. Table 11.2 shows the monthly distribution of the maximum 1-hour precipitation from the extreme storm database. The dominance of summertime storms (June, July, August) is clear and is strongly related to the seasonal heating maxima. Changery (1981) and Changnon (1988a

and 1988b) found a similar pattern in their studies of thunderstorm occurrences across the United States. Schaefer (1989), studying extreme rainfall events in Washington State, also found a strong summer maxima for short duration storms.

From an examination of the extreme storm database (Appendix 4), the diurnal frequency distribution of maximum 1-hour convective rainfall events was determined. The 2-hour period with the greatest number of occurrences ending at 1600 LST contained about 30 percent of all storms, while nearly 70 percent occurred during the period from 1400 to 2000 local time. Only 11 percent had maximum hourly rainfall between midnight and 1200 LST. The relative infrequency of nocturnal heavy thunderstorm activity is in distinct contrast to the

Table 11.2.--Monthly distribution of extreme local convective storms - Pacific Northwest.

Month	Frequency
May	7
June	31
July	32
August	32
September	4
October	1
Total	106

Source: Extreme local storm database (Appendix 4)

pattern over portions of the midwest (Wallace, 1975). The absence of a nocturnal low-level jet stream, an important factor in the nighttime frequency of thunderstorms in the Great Plains, contributes to the relative infrequency of heavy storms at night in the Pacific Northwest. A study of western region flash flood events using satellite imagery by Fleming and Spayd (1986), also found a strong link between solar heating and these storms. The Washington State study by Schaefer (1989) is in concurrence with this finding, with a strong afternoon maxima in the heaviest short duration storms.

The importance of divergence aloft has already been noted, but this process takes on added significance when there is concomitant low-level convergence. Low-level convergence in the form of lines, or boundaries or fronts, plays a crucial role in providing the mechanical lift necessary to bring air above the level of free convection (LFC). Terrain and boundaries are the most frequent causes of low-level convergence (House, 1963; Miller, 1967; McNulty, 1983). Low-level convergence produced by a storm's gust front may also play a critical role in the

cell redevelopment process for multicellular thunderstorm outbreaks (Weisman and Klemp, 1986).

Thunderstorms are generally classified into three basic types, single-cell, multicellular, and supercell (Browning, 1981; Doswell et al., 1990). There is a wide range of dynamic severity and precipitation intensity among these types, which of course affects the rainfall distribution. It appears that the latter two types are not frequently found in the Pacific Northwest region, especially compared to much of the eastern United States and even the southwestern United States. This conclusion is borne out by the studies of Fleming and Spayd (1986), and Maddox et al. (1980) on western United States flash flood events. In addition, mesoscale convective systems (MCS's) are comparatively infrequent across much of the western United States as discussed by Lussky (1986). The major limiting factor in preventing their occurrence seems to be the lack of a continuous source of warm, moist, unstable air feeding into the region.

11.2.3. Synoptic Study of Northwest Extreme Local Storms

Appendix 4 provides individual discussions on three extreme local storms occurring in the region and two storms that occurred near the region. Also included in this Appendix are the synoptic patterns common to most extreme convective events.

The analysis revealed that there clearly are preferred meteorological conditions under which extreme local storms develop in the Pacific Northwest. In the upper atmosphere (500-mb), the most dominant pattern conducive to the outbreak of extreme local rainfall, occurs when the station is located beneath the western side of a long-wave ridge (or east of a long-wave trough). The ascending motion characterizing the mid-tropospheric environment in these areas primes the atmosphere for convection. A short-wave perturbation moving up the ridge often aids in destabilizing the atmosphere in the vicinity. This pattern is similar to that most often found to cause flash flooding in the western United States (Maddox et al., 1980). Southerly winds associated with this pattern are also of importance in feeding the necessary moisture into the area. Other important factors operating at different scales also have an influence on the type and intensity of any storms that do develop.

Surface weather patterns favorable for local storm development are more variable than aloft, although low pressure-trough situations are most often associated with such storms. The salient point to be made in discussing heavy local storms in the Pacific Northwest is that they definitely occur under preferred synoptic conditions, but are influenced to a large degree by factors operating at the sub-synoptic and mesoscale area size as well.

11.3 Adjustment for Maximum Moisture

11.3.1 Background

Surface dew points are used as a measure of atmospheric moisture for local storms just as they are for general storms in this study. Virtually all previous PMP studies have used dew points as an indicator of atmospheric moisture, and numerous researchers have established the validity of this concept (Reitan, 1963; Berkofsky, 1967; and Bolsenga, 1965). It is especially important to have an accurate estimate of low-level moisture since it is this air which is drawn into the thunderstorm, lifted and condensed and finally falls as precipitation.

11.3.2 Maximum Persisting 3-Hour Dew Points

In this study, 3-hour 1000-mb maximum persisting dew points were used as a measure of atmospheric moisture for the maximization and transposition of local storms. All dew-point data were reduced pseudo-adiabatically to 1000-mb in order to account for variations in elevation and to provide a common level for comparison. Previous major studies (HMR 49 and 55A) have used 12-hour maximum persisting dew points for both general and local storm maximization. The 3-hour persisting dew point in a local storm situation may be higher than the 12-hour persisting dew point by several degrees (F) or more due to localized moisture convergence. McKay (1963) found that 3-hour maximum persisting dew points in the Canadian prairie provinces average about 4°F greater than the corresponding 12-hour maximum persisting dew points for dew points in the 55 to 75°F range, which are representative of high dew-point episodes. Consequently, a 3-hour maximum persisting dew point read as close as possible to the storm location better represents the localized moisture available for the storm than a 12-hour maximum persisting dew point, which would more accurately indicate the widespread moisture available for a general storm. Additionally, a high 3-hour persisting dew point is less likely to be the result of an erroneous observation, as is sometimes the case with an individual dew point measurement.

Maps of 3-hour maximum persisting local storm dew point at 1000-mb are shown for the Pacific Northwest region in Figures 11.2-11.8. They were drawn only for April through October because the extreme local storms of concern to this study occur during this period. The isolines depicted on these maps represent the broadscale moisture and temperature patterns affecting the Pacific Northwest. A brief discussion of these maps follows.

April, a transitional month from winter to spring, shows a nearly east-west orientation of the isolines. The moisture source at this time of year is almost exclusively the central or north Pacific Ocean due to the strong zonal flow that usually predominates across this area. Because there is only this single moisture source, the variation in persisting dew points across the region is quite low during this month, only about 7°F.

From May through July however, the increasing influence of both Gulf of Mexico and tropical Pacific moisture becomes evident as a less zonal upper-air flow takes hold across the region. This can be seen in the definite southwest to northeast orientation of the isolines. The persisting dew point variation across the region reaches a maximum of nearly 16°F during July, with a maximum 3-hour persisting dew point near 78°F in the extreme southeast. The northwestern sections of the region reach only the low 60's, indicating that tropical moisture rarely, if ever, penetrates this far north and west. Extreme local storms are most likely to develop during these months due to the increased moisture, less stable atmosphere and slow movement of thunderstorm cells.

September is somewhat of a transitional month, as the orientation of the isolines once again becomes more east-west and the regional variation diminishes to only 9°F. October shows a near reversal of the warm season pattern, as Gulf and tropical moisture sources are cut off with the stronger flow of autumn and polar air begins to intrude from the northeast, reducing the moisture bearing capacity of the atmosphere. The highest persisting dew points in this month are found in both the southwest and southeast and there is only a slight variation of about 5°F across the entire region.

11.4 Adjustments for In-Place Maximization

The in-place adjustment for moisture maximization of local-storm amounts is treated similarly to that for the general storm. A brief discussion of this process is given in Appendix 4 and it should be reiterated that the primary difference is in the use of 3-hour persisting dew points rather than the 12-hour persisting used in general storms. Moisture maximization is a ratio, and the use of 3-hour rather than 12-hour values, results in only minor differences, since the 3-hour persisting dew point analyses in this study roughly parallels the 12-hour persisting dew point patterns shown in HMR 43.

11.5 Adjustments for Elevation

The elevation adjustment used in local storms is the same as that described in Section 7.3 for the general storm with regard to vertical storm transposition. As described in somewhat greater detail in Appendix 4, available storm data, as well as literature, suggests that there is no evidence for variation in local-storm precipitation potential up to about 6,000 feet. Above this level, a decrease consistent with the reduction in available moisture is to be expected. This feature is consistent with the conclusion adopted in both HMR 49 and 55A.

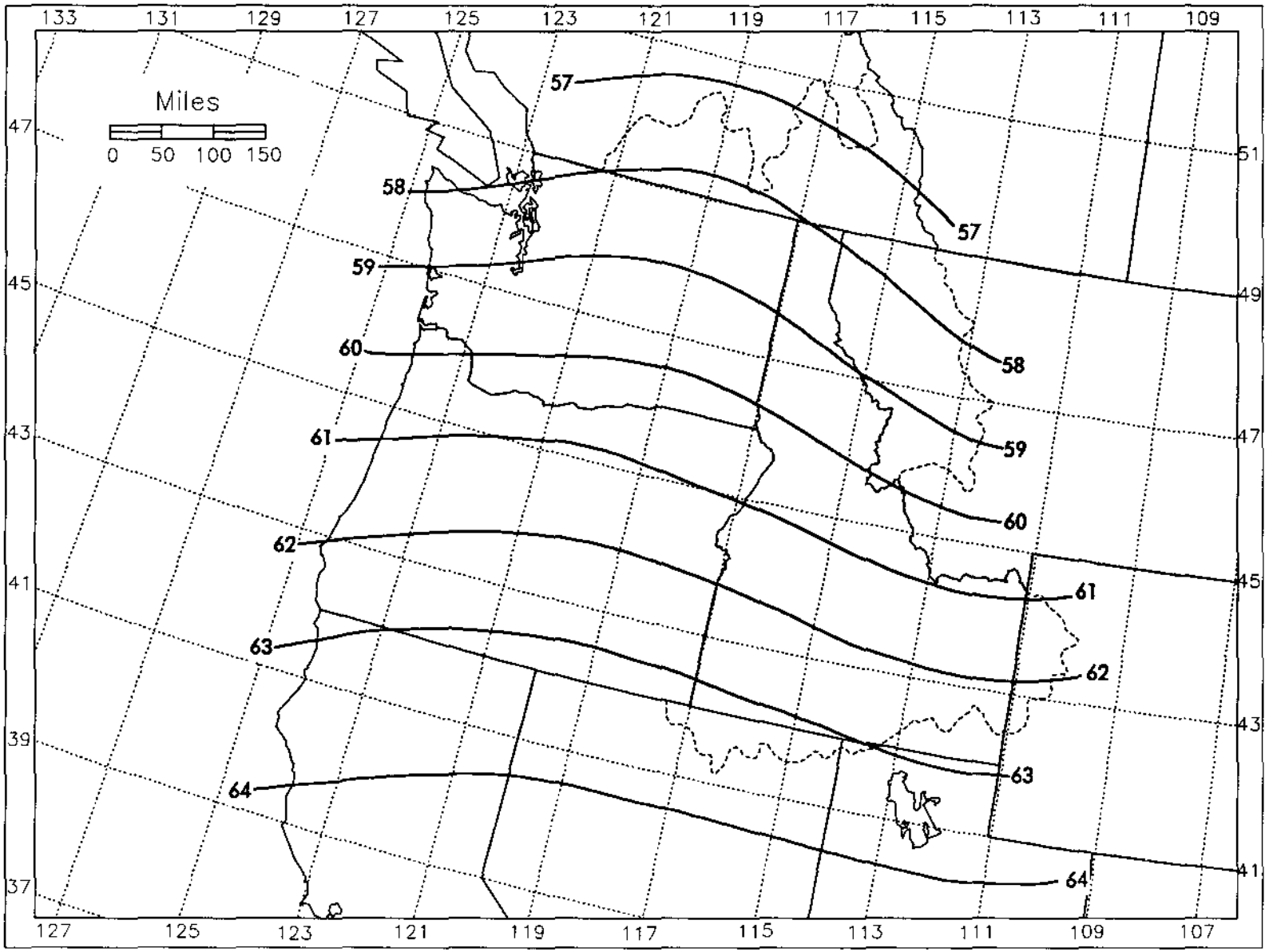

Figure 11.2.--Three-hour maximum persisting 1000 mb local storm dew points for April (°F).

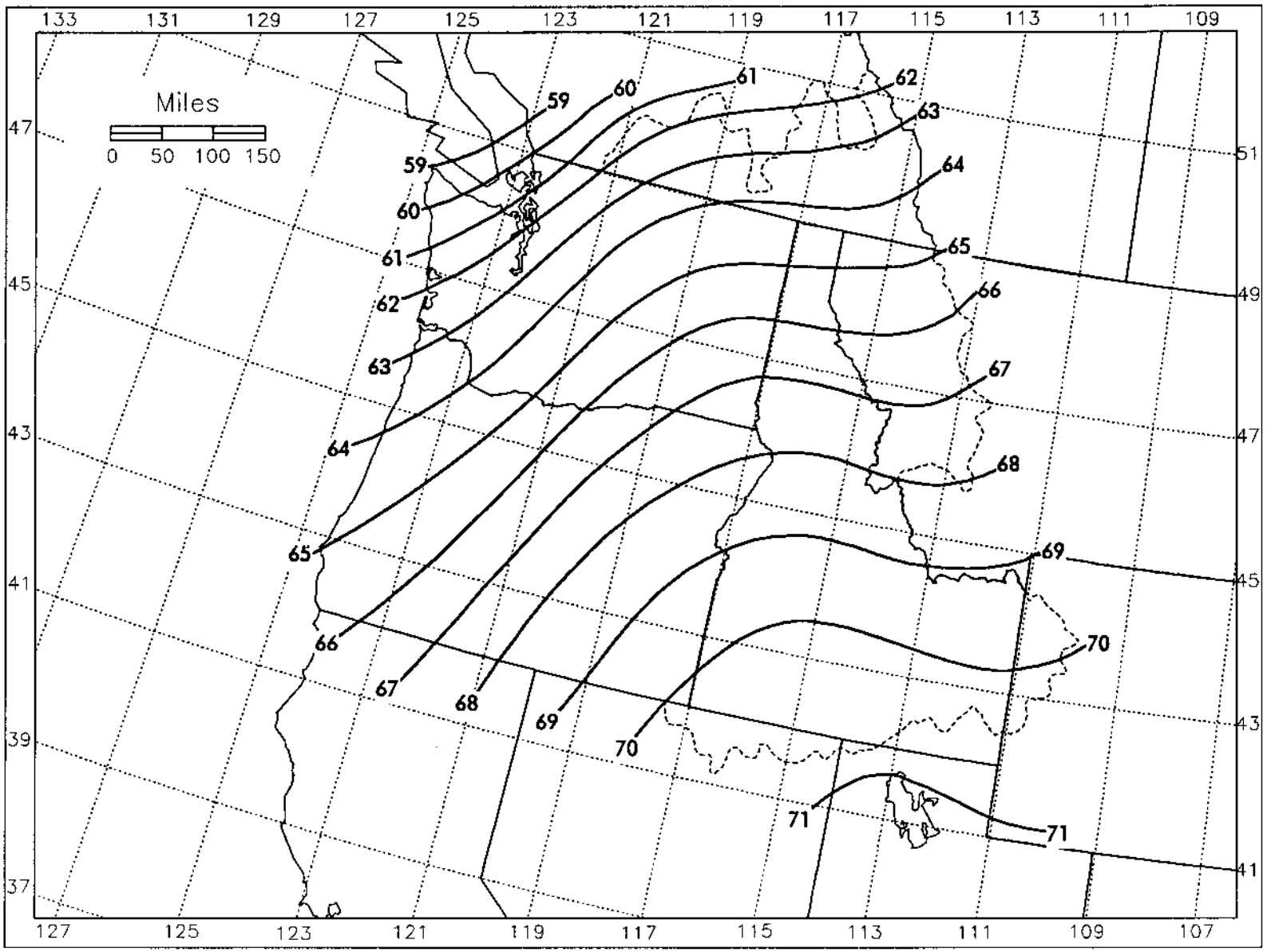

Figure 11.3.--Three-hour maximum persisting 1000-mb local storm dew points for May (°F).

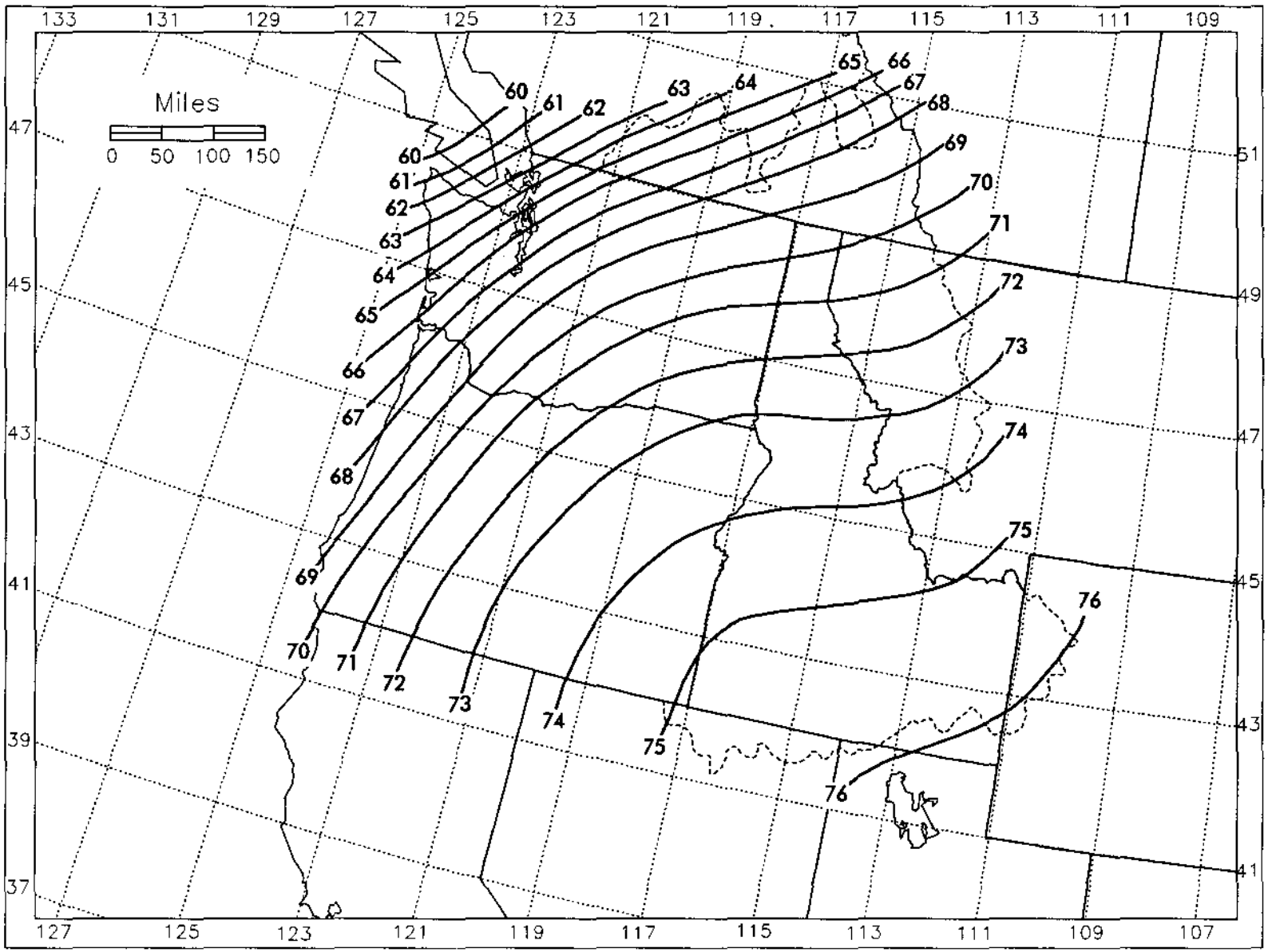

Figure 11.4.--Three-hour maximum persisting 1000-mb local storm dew points for June(°F).

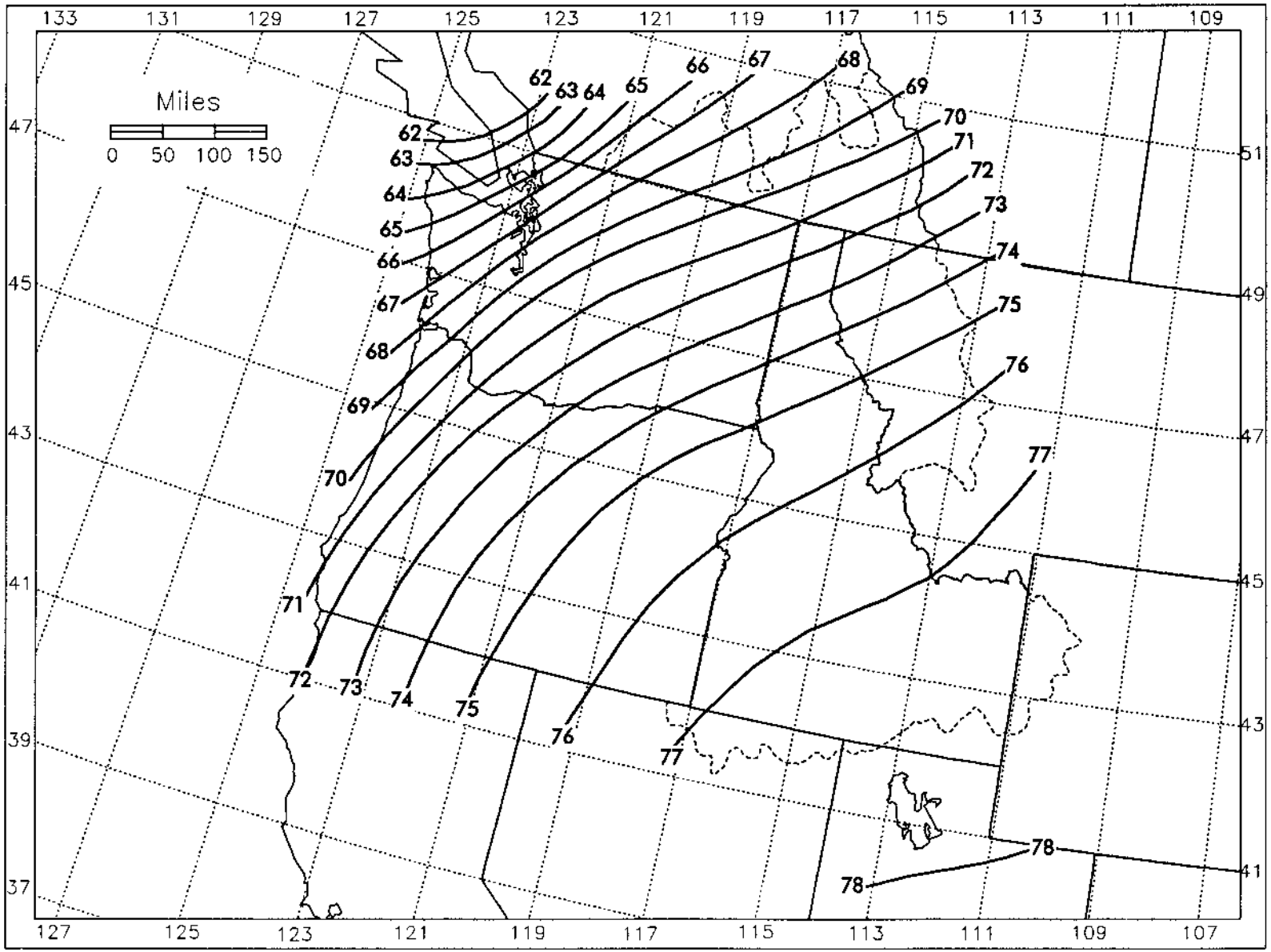

Figure 11.5.--Three-hour maximum persisting 1000-mb local storm dew points for July (°F).

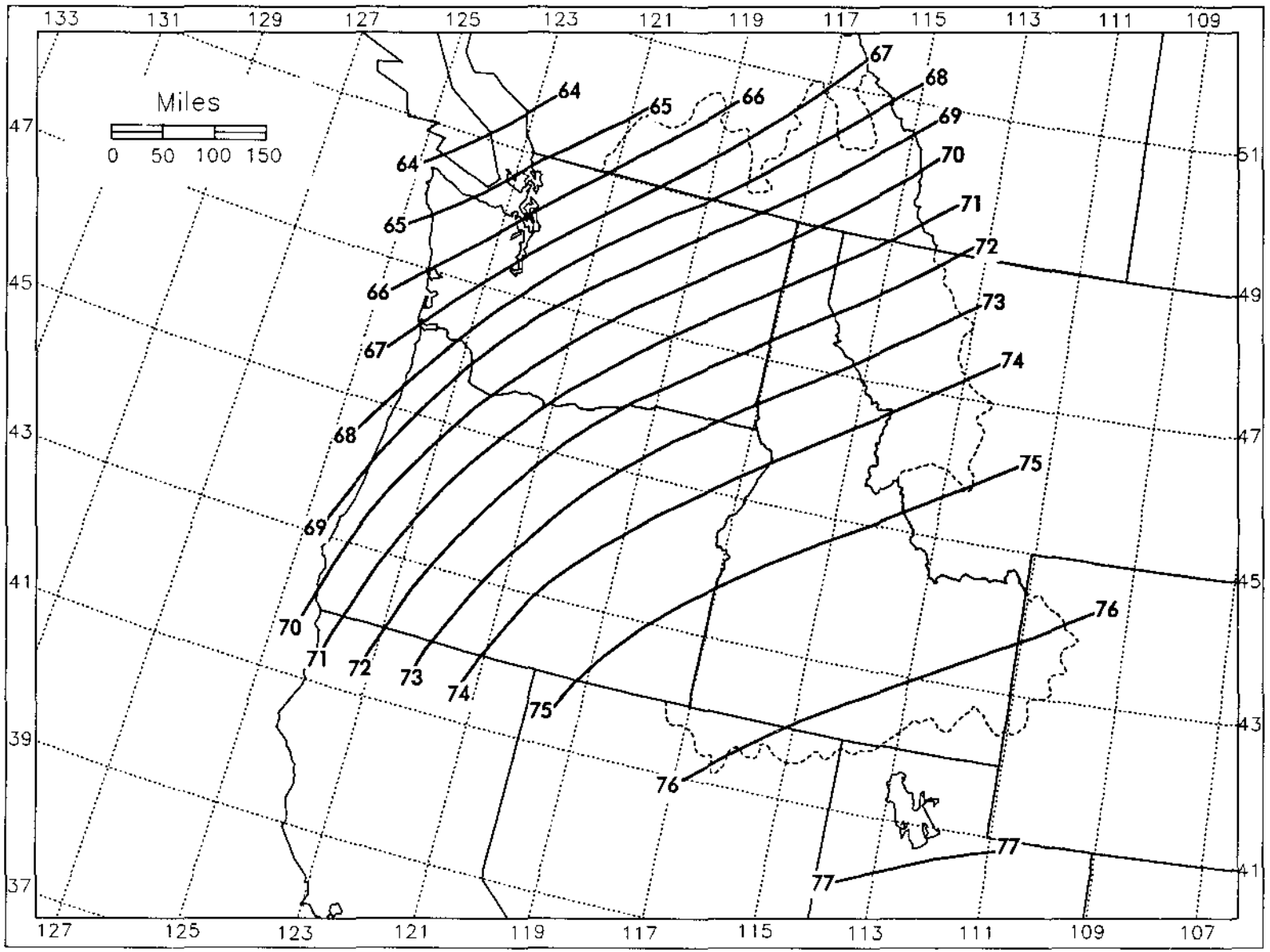

Figure 11.6.--Three-hour maximum persisting 1000-mb local storm dew points for August (°F).

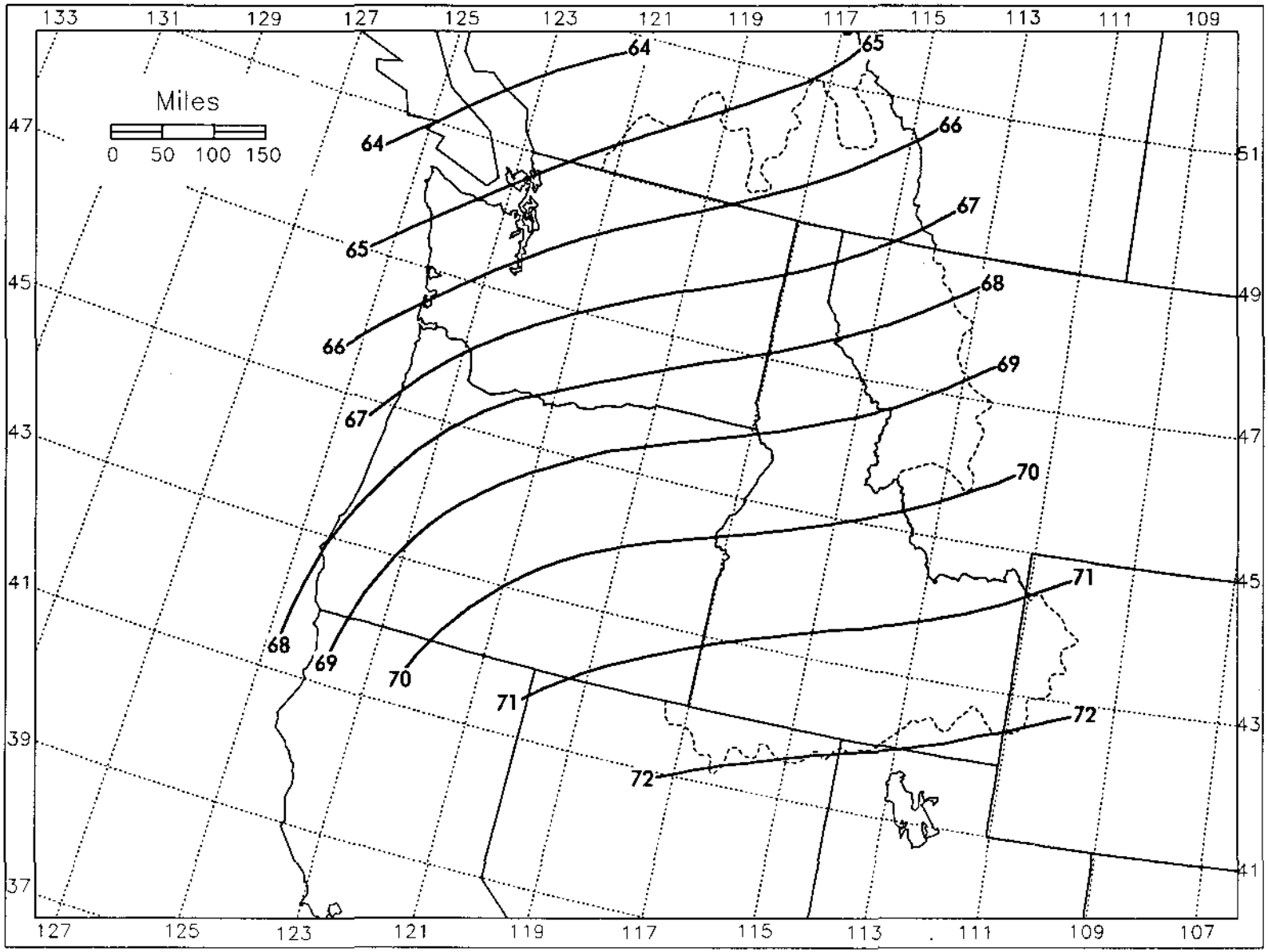

Figure 11.7.--Three-hour maximum persisting 1000-mb local storm dew points for September (°F).

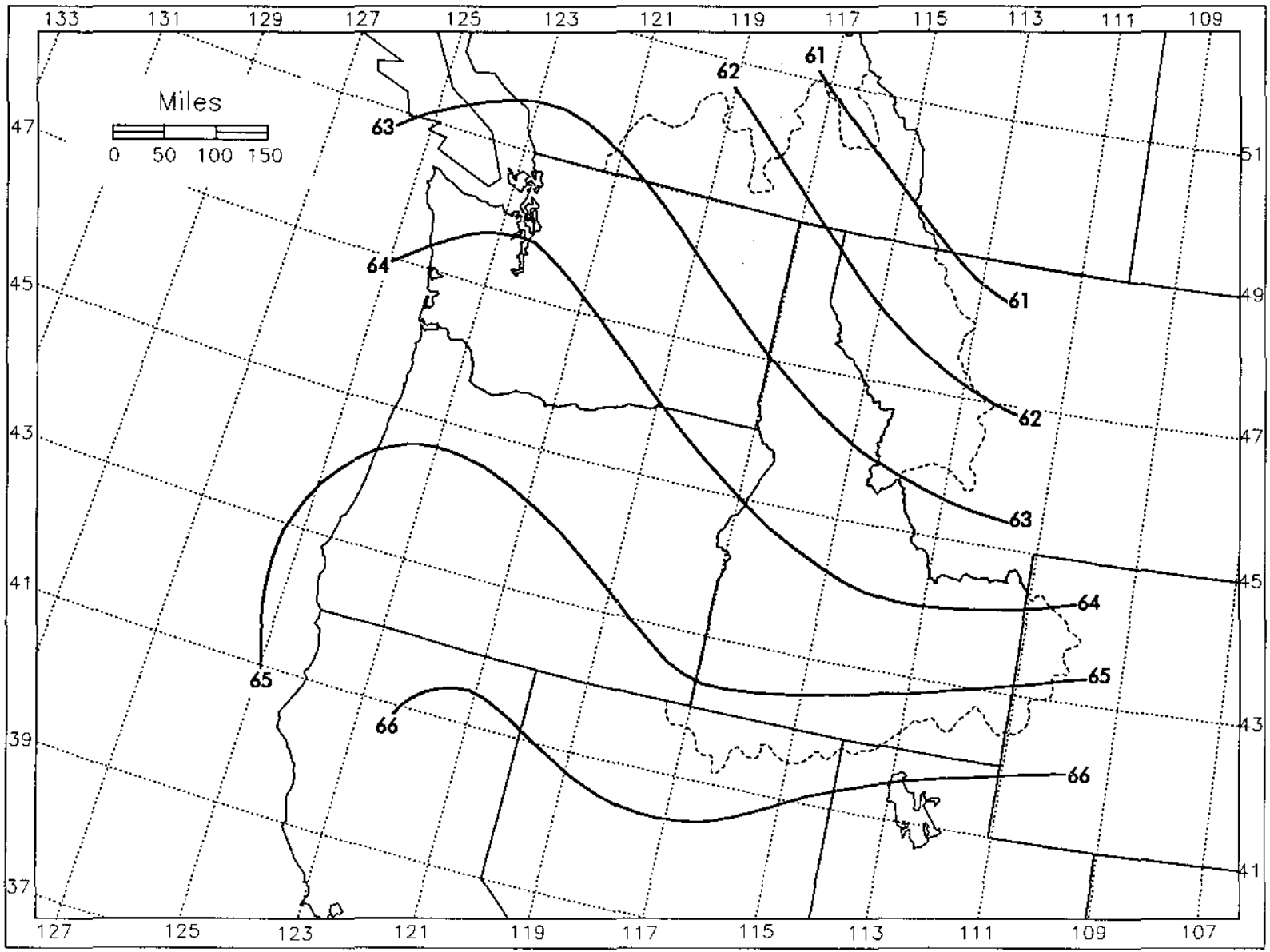

Figure 11.8.--Three-hour maximum persisting 1000-mb local storm dew points for October (°F).

11.6 Adjustment for Horizontal Transposition

Local storms were transposed in this study within the climatic zones discussed in Appendix 4, using procedures similar to those applied to the convergence component of general storms (see Section 7.4).

11.7 Durational Variation

11.7.1 Background

Research conducted into the nature of Pacific Northwest local storms has shown that they primarily draw on limited moisture, which has difficulty penetrating much of the region due to terrain obstacles. Lacking the constant replenishment of moisture, these local storms often produce their heaviest rainfall within the first hour, with total storm duration rarely exceeding 6 hours (Schaefer, 1989). For example, of the most extreme recorded local storms in Table 11.1, only two produced significant precipitation beyond 1 hour. These were the Elko, Nevada, storm of August 27, 1970 (3.47 inches in 1 hour, 4.13 inches in 4 hours) and the poorly documented John Day, Oregon, storm of June 9, 1969 (hourly precipitation unknown, 7 inches of precipitation reported in an estimated duration of 3 hours). The evidence indicates that Northwest local storm PMP would be expected to produce most of its precipitation within about the first hour.

11.7.2 Analysis

In HMR 43, a depth-duration relationship was derived from a plot of the greatest recorded local storms in and around the region, extrapolated to 6 hours. The curve was based on depth-duration data from less significant thunderstorms selected from United States Weather Bureau Technical Paper Number 15 (USWB, 1956). The 6/1-hour PMP ratio from that study was 1.43, a value which now appears to be too high based on the more recent data available for the current investigation (Vogel et.al., 1990; Schaefer, 1989).

A depth-duration plot of the greatest storms transposed to the Idaho/Oregon/ Nevada intersection was used to determine a depth-duration relationship for durations up to 1 hour (Figure 11.9). For longer durations (1 to 6 hours), there was no adequate storm sample available to explicitly determine a depth-duration relationship. In HMR 49, the durational variation was determined by an analysis of regionally averaged (within 2° latitude-longitude grid units) 6-/1-hour precipitation ratios for maximum clock-hour precipitation amounts. A similar analysis of 50-years or greater return period storms in the Northwest disclosed no discernible geographical pattern. Thus, no regional variation was utilized to describe the durational characteristics of local storms across the region.

One of the problems encountered in determining a 6-/1-hour precipitation ratio for local storm PMP involved the mechanics of such heavy storms. Due to the finite moisture supply usually available for local storms in this region, it is not at

all certain that the PMP storm will behave the same way as most observed heavy storms. The depletion of available moisture as it is converted into precipitation may be significantly faster in a PMP storm than most observed storms, leaving less moisture for a longer duration event. This is especially true where only limited moisture sources exist. Unfortunately, depth-duration data for local storms of near PMP magnitude do not exist to test this hypothesis in an explicit manner.

In an effort to gain some insight into the depth-duration characteristics of heavy storms, data from the extreme local storm database (Appendix 4) were examined. Of the 106 storms in this sample, 99 had durational information. The hourly precipitation occurring 6 hours before and after the maximum hourly amount was obtained for the 99 available storms. The duration distribution of these isolated convective storms is given in Table 11.3. These frequencies were derived from clock-hour samples and may be biased toward longer durations than actually occurred, as would show up more clearly using 5- or 15-minute data. More storms (30) had a duration of 2 hours than any other single duration, and 65 of the storms had a duration of 3 hours or less. Only 6 storms had a duration beyond 6 hours, and the precipitation amounts outside the maximum hour were minor for these 6 cases (Vogel et. al, 1990).

Table 11.3.--Frequency distribution of storm durations from the extreme local storm data base.

Duration (hour)	Frequency (number of events)
1	16
2	30
3	19
4	13
5	9
6	9
>6	6
Total	99

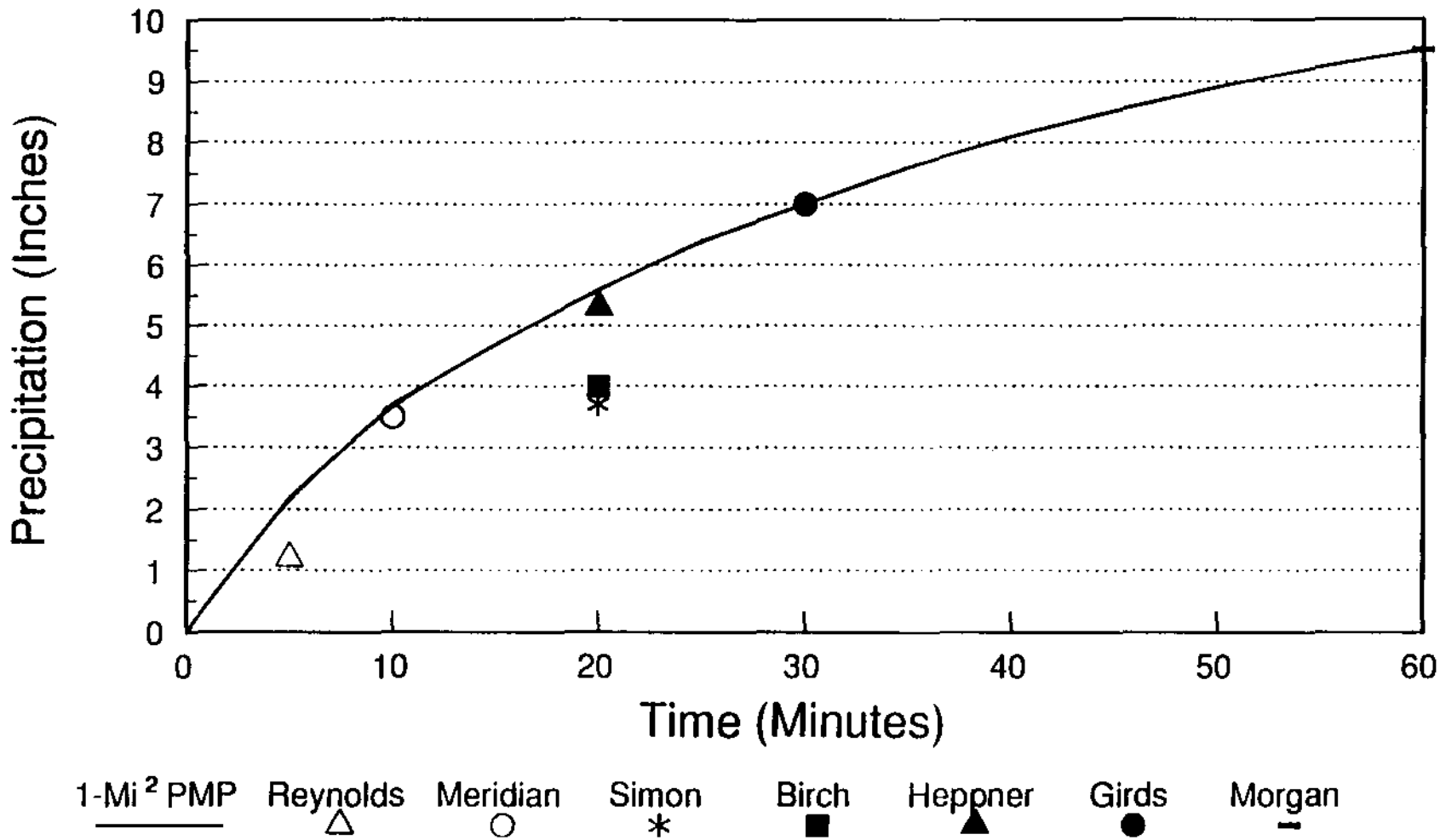

Figure 11.9.--1-mi² local storm PMP at the Idaho/Oregon/Nevada border.

No true median duration could be established for this data set, but it can be said that the median duration is 2 to 3 hours for heavy, convective storms in the Pacific Northwest. By comparison, Changnon and Vogel (1981) found that the median duration for heavy, convective rain intensities in Illinois was 3.2 hours, and durations on this order hold true for a large part of the eastern United States.

On average, the 6-hour to 1-hour ratio of rain is about 1.10 to 1.15 in the storms of the Pacific Northwest, which is considerably lower than the ratio of 1.4 found for general thunderstorms in the United States (USWB, 1947 and 1956) or compared to the 1.43 value adopted in HMR 43. The 1.10 to 1.15 values are closer to the results obtained by Schaefer (1989) in his study of heavy rainstorms in Washington State. That study, based on 2-hour extreme storms, found 6/1-hour ratios that varied between 1.01 for an exceedance probability of 0.15 (see Chapter 10) in eastern Washington to about 1.12 for the same probability in western Washington. Figure 11.12 and Table 11.4 show the adopted depth-duration ratio expands only to 1.15 for the entire Northwest region.

11.7.3. Temporal Variation

The 99 storms in the Northwest were further classified into front-, middle-, and end-loaded storms, depending upon the timing of the maximum precipitation. This classification scheme depends upon the duration of the local storm. For example, a storm with a 6-hour duration would be divided into three 2-hour segments. The 2-hour segment with the greatest precipitation amount would define whether the storm is front-, middle- or end-loaded. If the greatest precipitation is in the first two hours, then the storm is front loaded; if the greatest precipitation amount occurred in the third and fourth hours, then the storm would be middle-loaded. For a storm with a 60-minute duration, the storm would be divided into three 20-minute segments. Then if the greatest precipitation is between 20 and 40 minutes of the storm, it would be a middle-loaded storm. Thus, front-, middle- and end-loaded storms are defined by the highest rainfall amount within either the first, second, or last third of the duration of the storm. Since 1972, Fischer-Porter raingages, with 15-minute amounts, have allowed 1 or 2-hour duration storms to be classified in this way. Under this classification scheme, about 65 percent of the 99 storms considered in this study were front-loaded, 33 percent were middle-loaded and only 2 percent were end-loaded. The predominance of front- and middle-loaded extreme convective storms in the Pacific Northwest is clearly indicated by these data. The temporal distribution of the rainfall within these storms was examined using the techniques similar to those developed by Huff (1967). Figures 11.10 and 11.11 give the temporal distribution of precipitation for front- and middle-loaded storms in this study, while end-loaded storms were not considered due to their rarity. In both the front- and middle-loaded storms over 70 percent and often 90 to 100 percent of all rain occurs in 1 hour or less. A study by Farmer and Fletcher (1972) using data from two dense raingage networks in the Great Basin of Utah disclosed similar results. The most intense rainfall bursts in their studies occurred in the first quartile of storms about 80 percent of the time.

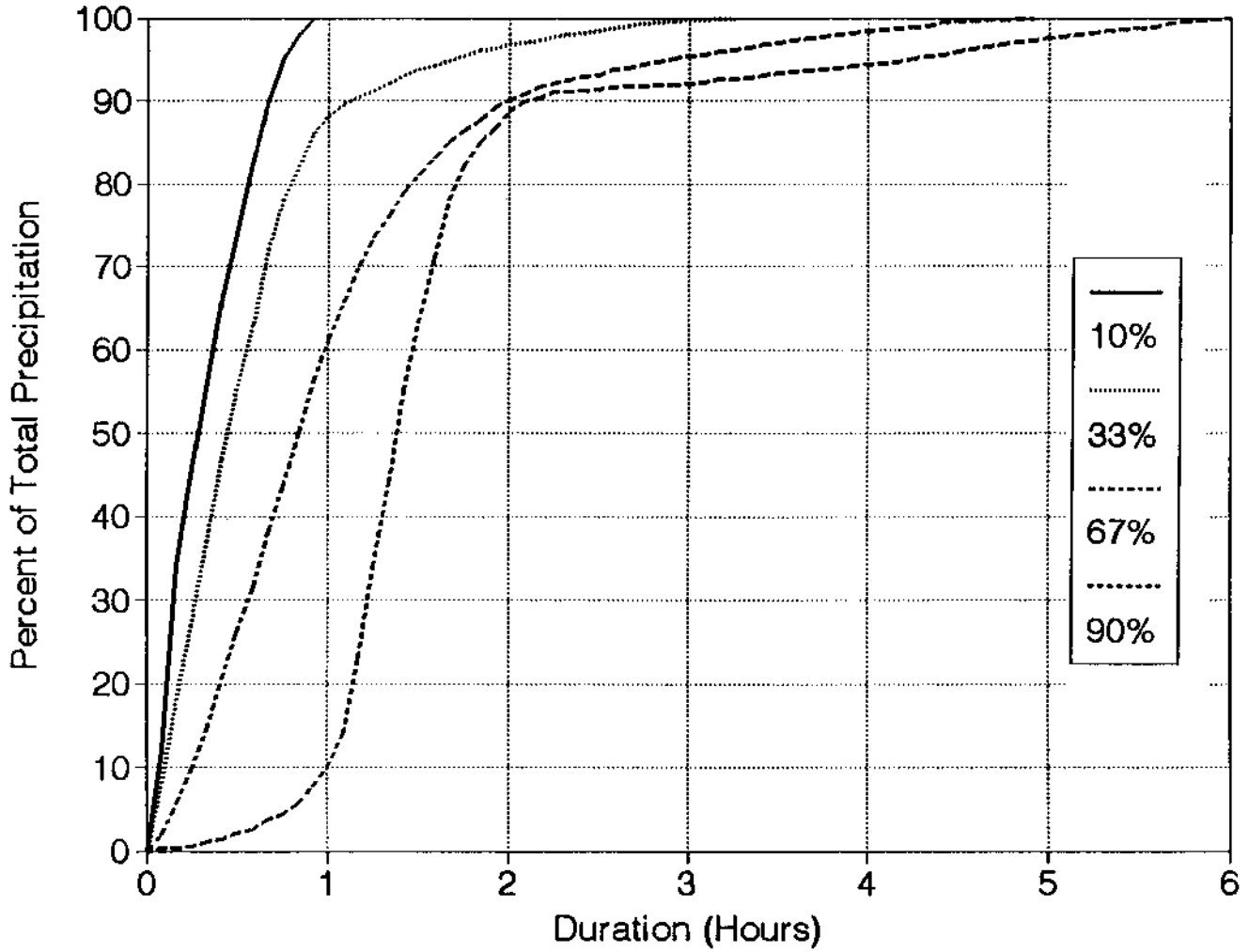

Figure 11.10.--Representative time distributions for front-loaded storms.

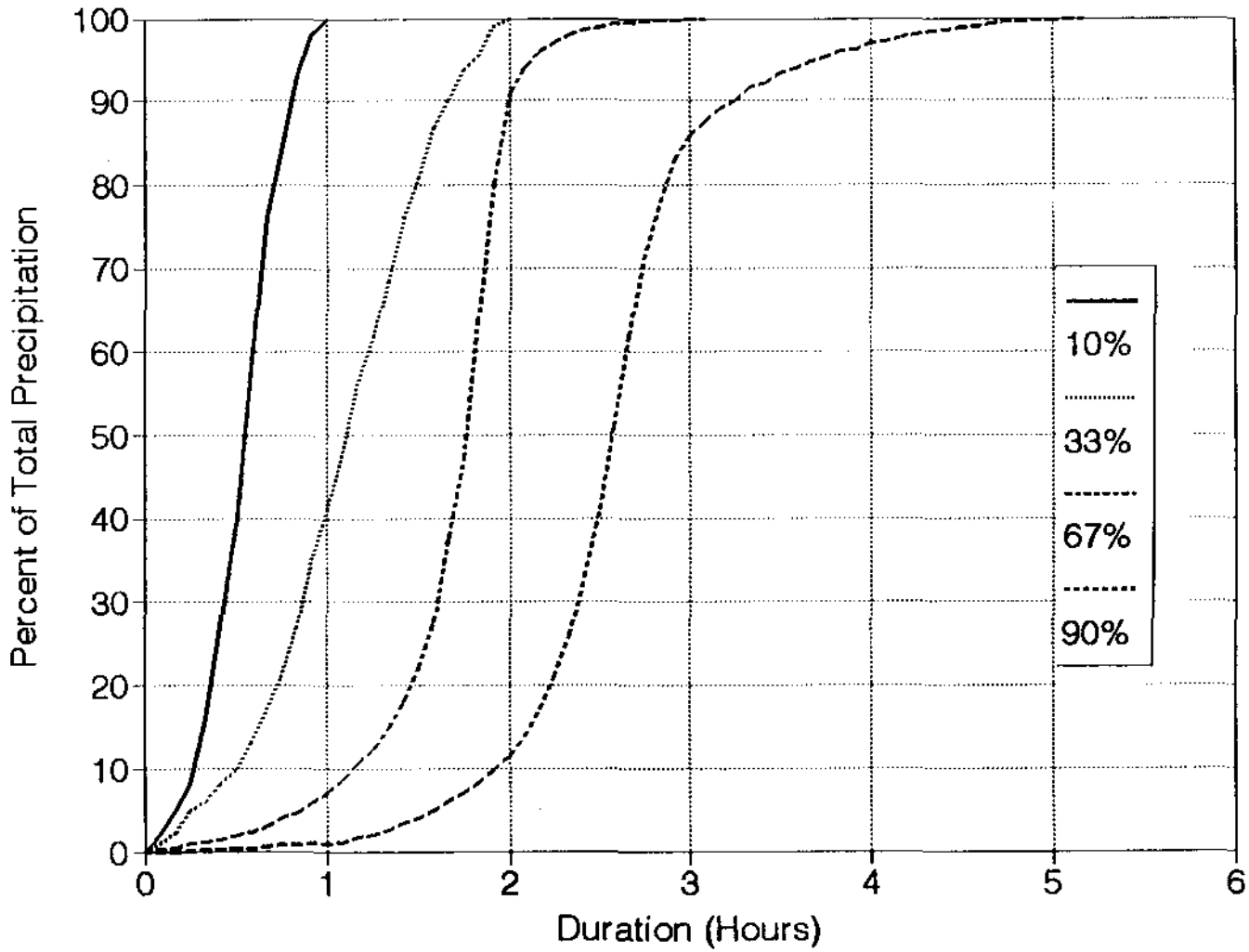

Figure 11.11.--Representative time distributions for mid-loaded storms.

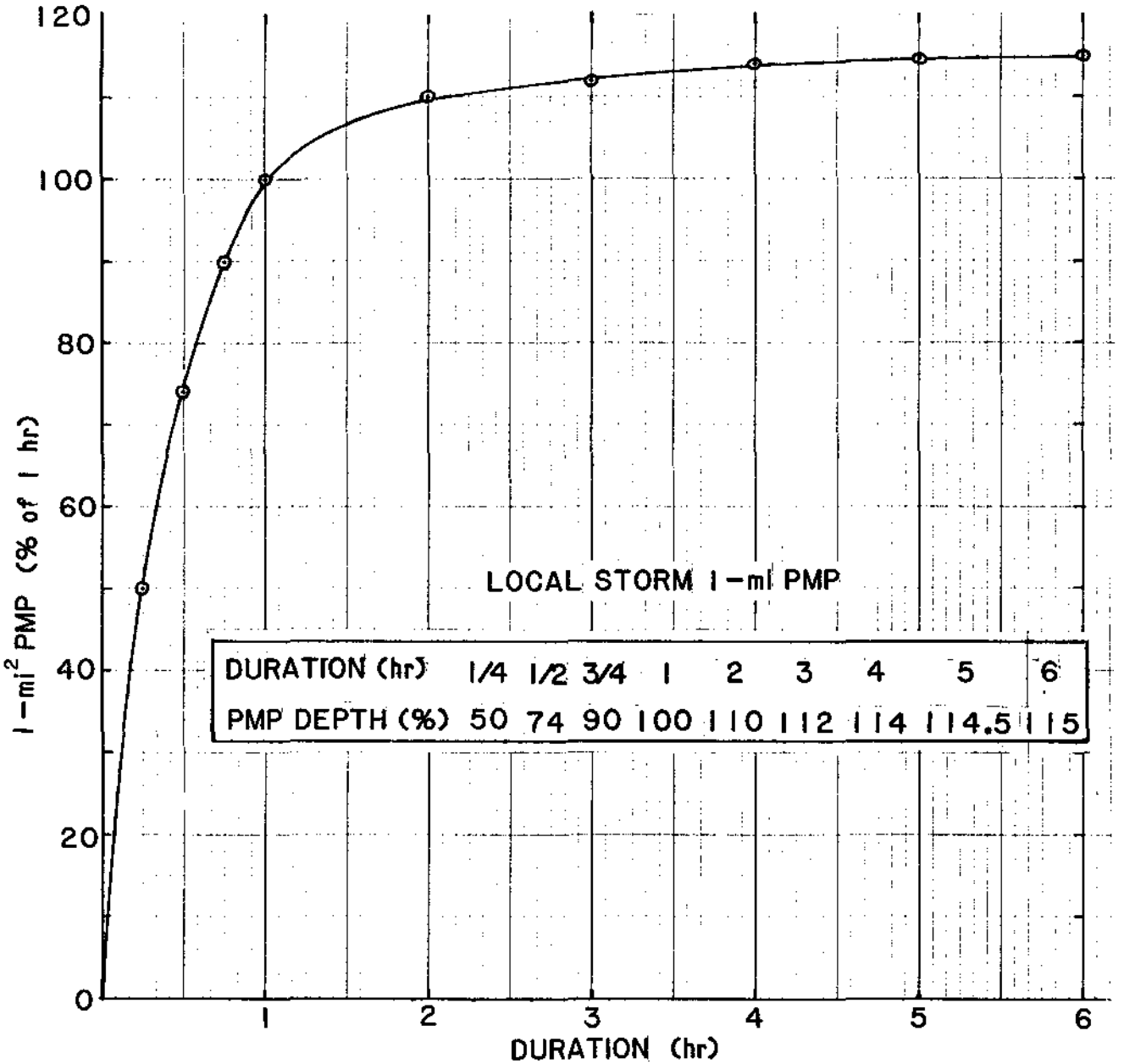

Figure 11.12.--Depth-duration relationship for 1-mi² PMP Pacific Northwest States.

Table 11.4.--Percent of 1-hour, 1-mi^2 local storm PMP for selected durations in the Pacific Northwest.	
Duration	Percent of 1-hour PMP
15 min	50
30 min	74
45 min	90
1 hour	100
1 hour, 30 min	107
2 hours	110
3 hours	112
4 hours	114
5 hours	114.5
6 hours	115

11.8 Depth Area Relations

11.8.1 Background

The index values (Figure 11.19) for local-storm PMP have been developed for an area size of 1-mi^2. PMP estimates for larger areas, up to 500-mi^2, also need to be developed. The index values can then be related to the average depth over a specified area at various durations.

Since the behavior of extreme local storms affecting the Pacific Northwest is different from those in the eastern United States, a review was made of Northwest data to find information more representative of the region. Previous PMP studies have used data from a number of different sources for the development of depth-area curves.

The depth-area curves developed in Technical Paper (TP) 29 (USWB, 1957-60), represented one of the early attempts to derive depth-area relations for small area watersheds (<500-mi^2). In TP 29, data were obtained from 20 dense raingage networks covering areas up to 400-mi^2 located in the eastern half of the United States and along the west coast. Only 2 of the 20 networks were located in the Pacific Northwest, with an additional 5 located in California. These curves

became known as the National Average Depth-Area Curves and were also used in later precipitation-frequency studies, TP 40 (Hershfield, 1961) and NOAA Atlas 2 (Miller et al., 1973).

HMR 43, adopted depth-area relations based on a compromise between (1) eastern type thunderstorms, (2) data from a few intense thunderstorms west of the Continental Divide, and (3) a model thunderstorm.

In the report for the Colorado River and Great Basin drainages (Hansen et al., 1977), PMP depth-area relations were based on data from southwest rainfalls and consideration of a model thunderstorm. The adopted curves in that study envelop both the data and the model thunderstorm curves. These curves were then used for both the 1- and 3-hour durations. For 6 hours, the relations developed in HMR 43 were accepted. Figure 11.13 shows area reduction curves from HMR 43 and HMR 49.

For HMR 55A, which examined the area between the Continental Divide and the 103rd meridian (Hansen et al., 1988), new depth-area data were available for only two local storms. Therefore, information from HMR 49 was used to supplement that study. This solution was warranted because of the geographic proximity of the HMR 49 area and the similar behavior of local storms to the east in terms of storm types, 6-/1-hour ratios, and terrain.

Another study which addressed the issue of local storm depth-area relationships was documented by Osborn et al. (1980) in which new depth-area curves for Arizona and New Mexico were developed. Regional data was believed to provide a better representation of depth-area relations in the southwestern United States and similar climates than the National Average Depth-Area Curves. Results showed that precipitation diminished faster with area than the National Average Depth-Area Curves. Osborn's curves are believed to be typical of summer thunderstorm rains in southwest Arizona.

Schaefer (1989) noted that a lack of recording precipitation gages in eastern Washington State made it impossible to determine new depth-area relations. Instead, he modified slightly the curves from HMRs 43, 49, and 55A for use in Washington. The major change suggested by Schaefer was that the maximum areal coverage for a 2-hour storm is only 250-mi^2. However, these curves are for storms that are less intense than PMP events.

11.8.2 Additional Depth-Area Analysis

An attempt was made in this study to derive new depth-area relations using precipitation records of a dense recording raingage network in southwestern Idaho. These records consisted of breakpoint data from the Reynolds Creek Experimental Raingage Network in southwestern Idaho for the years 1962-1988. Breakpoint data is precipitation intensity dependent data, in which starting and ending times for a specific intensity are given.

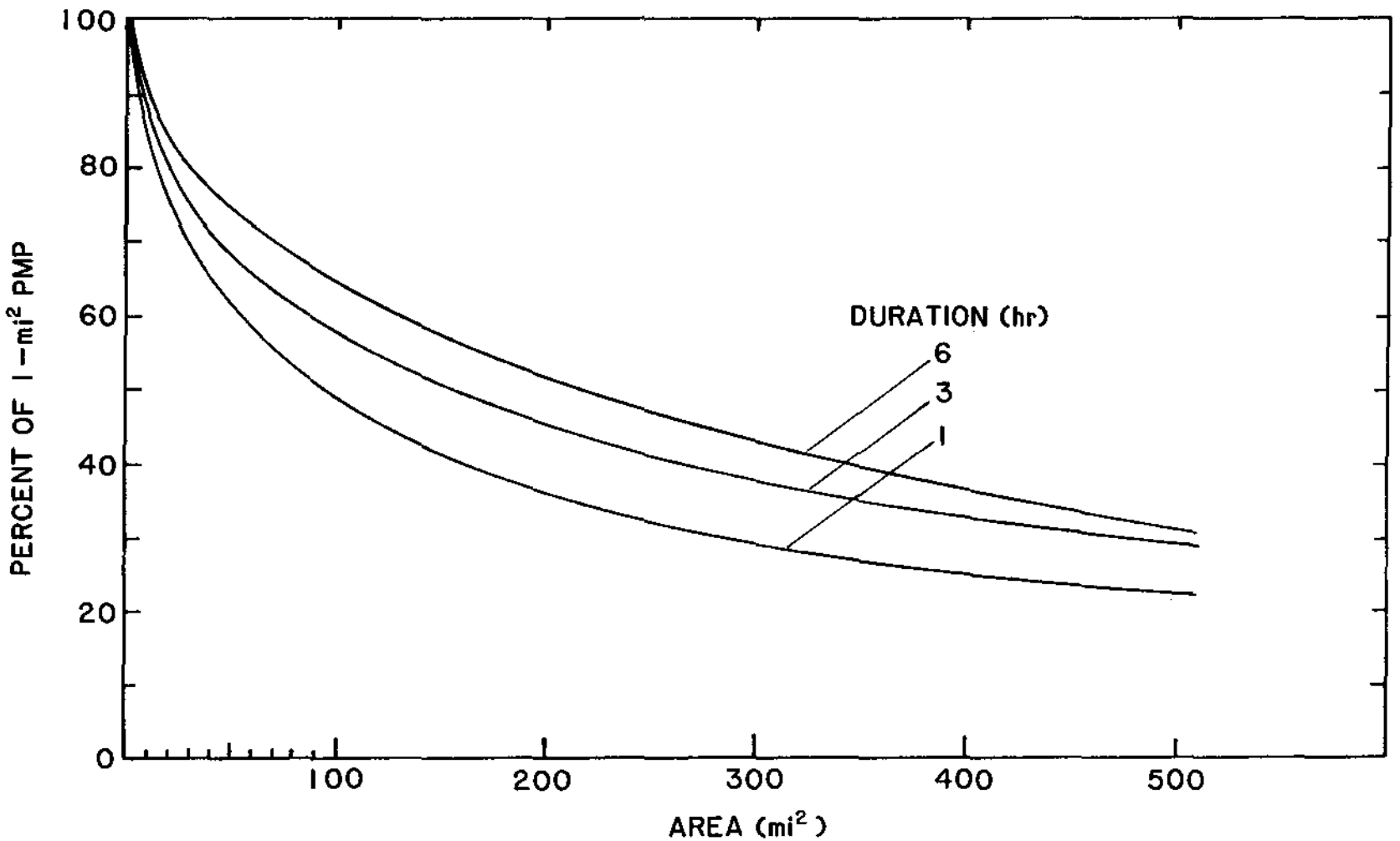

Figure 11.13.--Depth-areal relation for thunderstorm PMP in HMR 43 and 49.

The Reynold's Creek network is located on a 90-mi^2 watershed situated in the Owyhee Mountains about 50 miles southwest of Boise, Idaho. It is positioned at the headwaters of a north-flowing tributary of the Snake River. The elevation ranges from 3,600 to 7,200 feet above sea level with isolated peaks a few miles to the south and west rising to 8,000 feet. The network has an average density of one gage per 2-mi^2, and has varied over time between 12 and 31 gages.

A total of 587 station years of data were available for analysis. Only significant (>0.5 inches in 24 hours) local-storm data from April through October were selected for analysis. For each qualifying storm, a series of depth-area curves were created. Each curve was normalized by dividing the point rainfall amount by the largest (storm center) amount. This gives a Total Area Rainfall (TAR) ratio, and the curve that appears the flattest means a larger area received the bulk of the rainfall. Figure 11.14 shows normalized depth-area curves for the most significant storms, with the storm of July 21, 1975, clearly the most important. Several other storms also had relatively low TAR ratios, but were not as important due to their lower total rainfall amounts.

Figure 11.15 shows that the 1-hour curve from the July 21, 1975 storm varies only slightly from the depth-area curves from NOAA Atlas 2 up to 8-mi^2, then drops off appreciably at greater areas. The extremely localized nature and short duration of this storm provided insufficient justification to consider revising the overall depth-area curves from HMR 43 or HMR 49. Because not enough additional network raingage data and bucket surveys are available in the Pacific Northwest, no changes were warranted at this time. As a result, it was decided that the basic 1-hour curve used in HMR 49 is still considered valid (Figure 11.13).

11.8.3 Areal Distribution Procedure

Depth-area relations represent the average depth of precipitation (or PMP) for the respective area chosen. However, when one considers the areal distribution, the question that is asked is how should the precipitation be distributed (according to some selected isohyetal pattern) such that the same average depth is maintained. That is, assuming the precipitation falls as a single-centered storm, the areal distribution should have a maximum that is greater than the average depth given by the depth-area relation, and the minimum should be lower toward the periphery of the storm area size than the average depth. To answer this question, a rainfall pattern needs to be determined first. That is, the shape of the pattern and the distribution (number and gradient) of isohyets need to be fixed. Second, a set of depth-area relations and corresponding rainfall profiles need to be determined. If one starts from scratch, these depth-area relations may be patterned after average storm relations or from a specific controlling storm. The rainfall pattern can be circular or elliptical, concentric or eccentric. For this study, we chose the isohyetal pattern given in Figure 11.17 as being most representative of local storms applicable in the Northwest. This pattern is taken

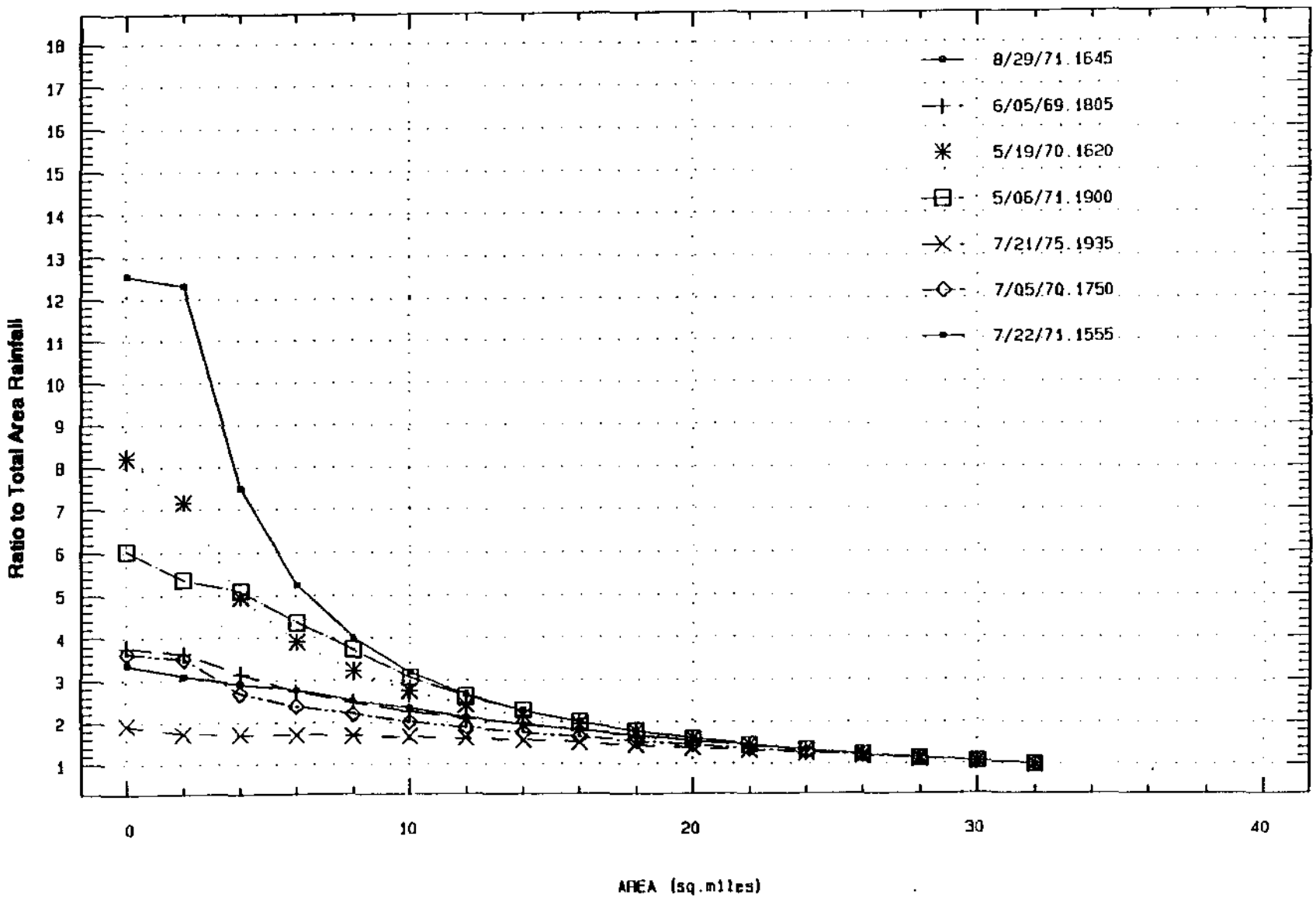

Figure 11.14.--Normalized 60-minute depth-area curves from Reynolds Creek dense network.

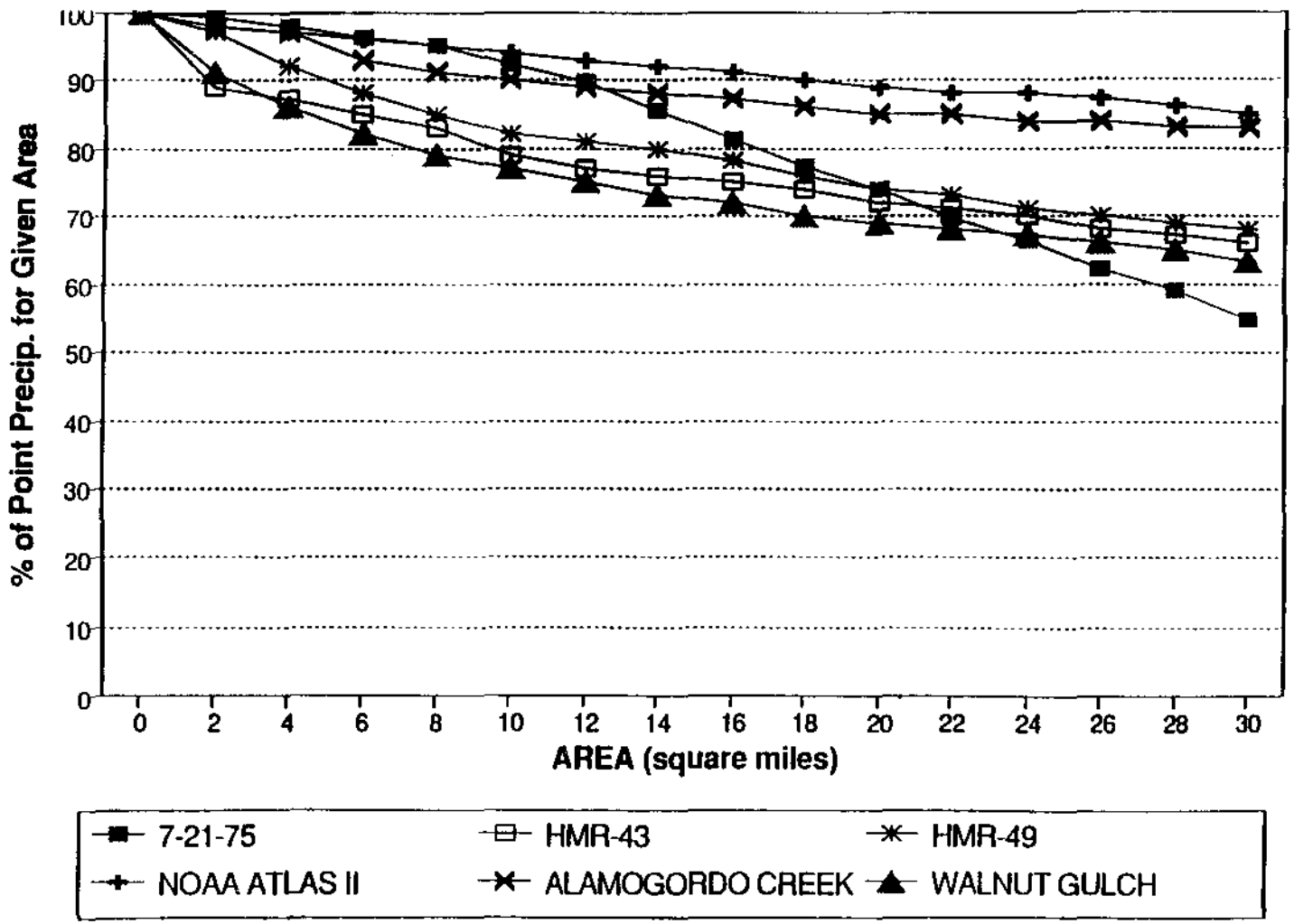

Figure 11.15.--Depth-area curve comparisons for 1 hour.

directly from HMR 49 (Figure 4.10 of that report). The isohyets (A to J) cover 500-mi^2 and were selected to provide a good representation through the pattern.

HMR 49 provides for multiple depth-duration curves (refer to Figure 4.3 from that publication). For the present study, we selected the adopted 1-mi^2 depth-duration curve from Figure 11.12 and compared it with the shape of a comparable 6/1-hour ratio curve from HMR 49 in Table 11.5. The HMR 49 curve shows considerably more intense convection, yielding higher short-duration ratios. We accept the depth-duration curve in Figure 11.12 as being more representative for this study region and maintain that data considered in this study suggest little to no variation through the region. Schaefer (personal communication, 1992) indicated that his data support different curves east and west of the Cascade Mountains. No resolution of this discrepancy was reached and further study in this area is recommended.

Table 11.5.--Comparison between 1-mi^2 depth-duration curve adopted for this study and that from HMR 49.

Duration (hour)	1/4	1/2	3/4	1	2	3	4	5	6
Depth (Figure 11.12) (% of 1 hour)	50	74	90	100	110.0	112.0	114.0	114.5	115.0
HMR 49 (for comparison)	80	91	96	100	108.5	112.0	114.0	114.5	115.0

The next step is to determine a 1-hour depth-area curve from storms or other sources. We adopted the 1-hour curve from HMR 49, which effectively is the same as the curve in HMR 43, as the basic depth-area relation for this study (Table 11.6).

Table 11.6.--One (1) hour depth area relation from HMR 43 as a percent of 1-mi^2 amount.

Area (mi^2)	1	5	10	50	100	200	300	400	500
Depth (% of 1-mi^2)	100	89.5	82.5	61.0	48.5	36.0	29.0	25.0	22.0

Finally, it was useful to determine the "equivalent radius" of each isohyet (equivalent implies that the area enclosed is equivalent to that for a circle). This simplifies the process when patterns other than circles are considered.

Table 11.7.--Equivalent radius in miles for selected areas representing areal pattern shown in Figure 11.16.

Isohyet	A	B	C	D	E	F	G	H	I	J
Enclosed Area (mi^2)	1	5	25	55	95	150	220	300	385	500
Equiv. Radius (mi)	.564	1.25	2.82	4.18	5.50	6.91	8.37	9.77	11.07	12.62

The computational procedure leads to determining the profile[1] that corresponds to the depth-area curve. The results of this procedure produce a precipitation profile curve for 1 hour that corresponds to a specific depth-area curve. Both relations can be plotted and smooth curves drawn for each. The plot for the profile curves should be in percent of 1-mi^2 versus equivalent radius, as shown for three curves in Figure 11.17. These plots can be on linear or semi-log paper. The semi-log plot accentuates the smaller areas/equivalent radius, where the largest variation generally occurs.

The 1-hour relation is considered fixed and all other durations are then related to the 1-hour curve. The incremental values in Table 11.8 have been determined from smoothing the curves in HMR 49, and are used to check durational and areal consistency.

[1]Profile refers to a cross section through the volume of precipitation that falls within a specific time period. A precipitation profile curve always falls off more rapidly than does the corresponding depth-area curve.

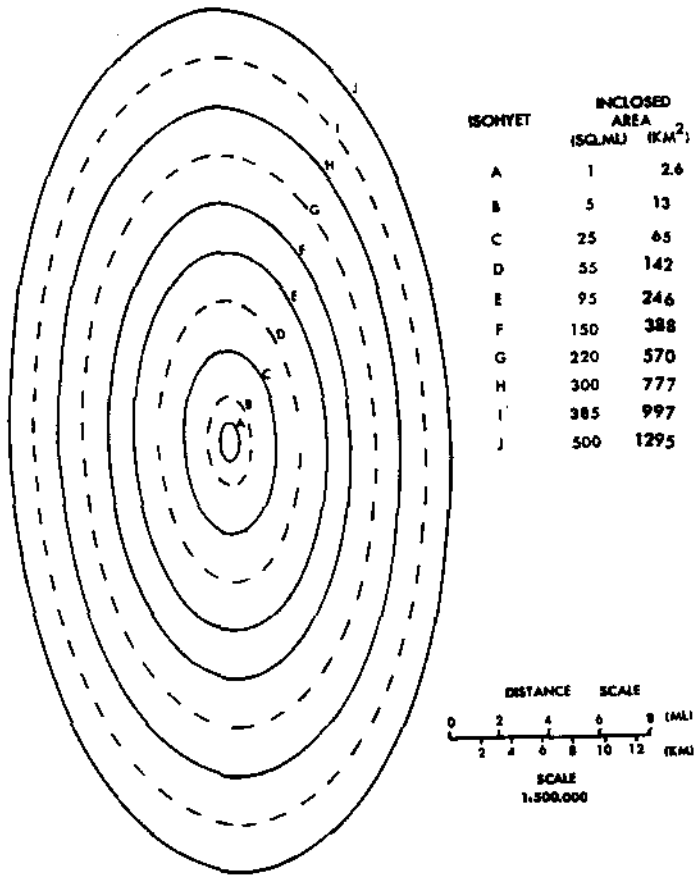

Figure 11.16.–Idealized local-storm isohyetal pattern (from HMR 49) used in this study.

Table 11.8--Incremental Profile (% of 1-hour, 1-mi² amount).									
	Duration (hours)								
Isohyet	1/4	1/2	3/4	1	2	3	4	5	6
A	-24.0	-16.0	-10.0	100.0	10.0	2.0	2.0	0.5	0.5
B	-21.0	-14.0	-7.8	74.8	8.7	2.0	2.0	0.5	0.5
C	-16.0	-11.5	-6.0	56.0	7.0	2.0	1.0	0.5	0.5
D	-11.5	-9.5	-5.0	43.0	5.0	1.5	1.0	0.5	0.5
E	-9.0	-7.0	-4.2	32.2	4.8	1.0	0.5	0.5	0.5
F	-6.5	-5.0	-3.4	22.4	2.6	0.7	0.7	0.5	0.5
G	-3.5	-3.5	-2.0	14.0	2.2	0.5	0.5	0.5	0.5
H	-1.5	-1.5	-1.5	6.5	1.8	0.5	0.5	0.5	0.5
I	-0.3	-0.3	-0.2	1.2	1.0	0.5	0.5	0.5	0.5
J	-0.1	-0.1	-0.1	0.5	0.5	0.5	0.5	0.5	0.5

From the incremental results given above, a new table of precipitation values can be derived from the 1-hour curve as the accumulated values in Table 11.9. Note that the A-isohyet percentages are those given in Table 11.4.

Table 11.9--PMP Profile Values (cumulative % of 1-hour, 1-mi² amount).									
	Duration (hours)								
Isohyet	1/4	1/2	3/4	1	2	3	4	5	6
A	50.0	74.0	90.0	100.0	110.0	112.0	114.0	114.5	115.0
B	32.0	53.0	67.0	74.8	83.5	85.5	87.5	88.0	88.5
C	22.5	38.5	50.0	56.0	63.0	65.0	66.0	66.5	67.0
D	17.0	28.5	38.0	43.0	48.0	49.5	50.5	51.0	51.5
E	12.0	21.0	28.0	32.2	37.0	38.0	38.5	39.0	39.5
F	7.5	14.0	19.0	22.4	25.0	25.7	26.2	26.7	27.2
G	5.0	8.5	12.0	14.0	16.2	16.7	17.2	17.7	18.2
H	2.0	3.5	5.0	6.5	8.3	8.8	9.3	9.8	10.3
I	0.4	0.7	1.0	1.2	2.2	2.7	3.2	3.7	4.2
J	0.2	0.3	0.4	0.5	1.0	1.5	2.0	2.5	3.0

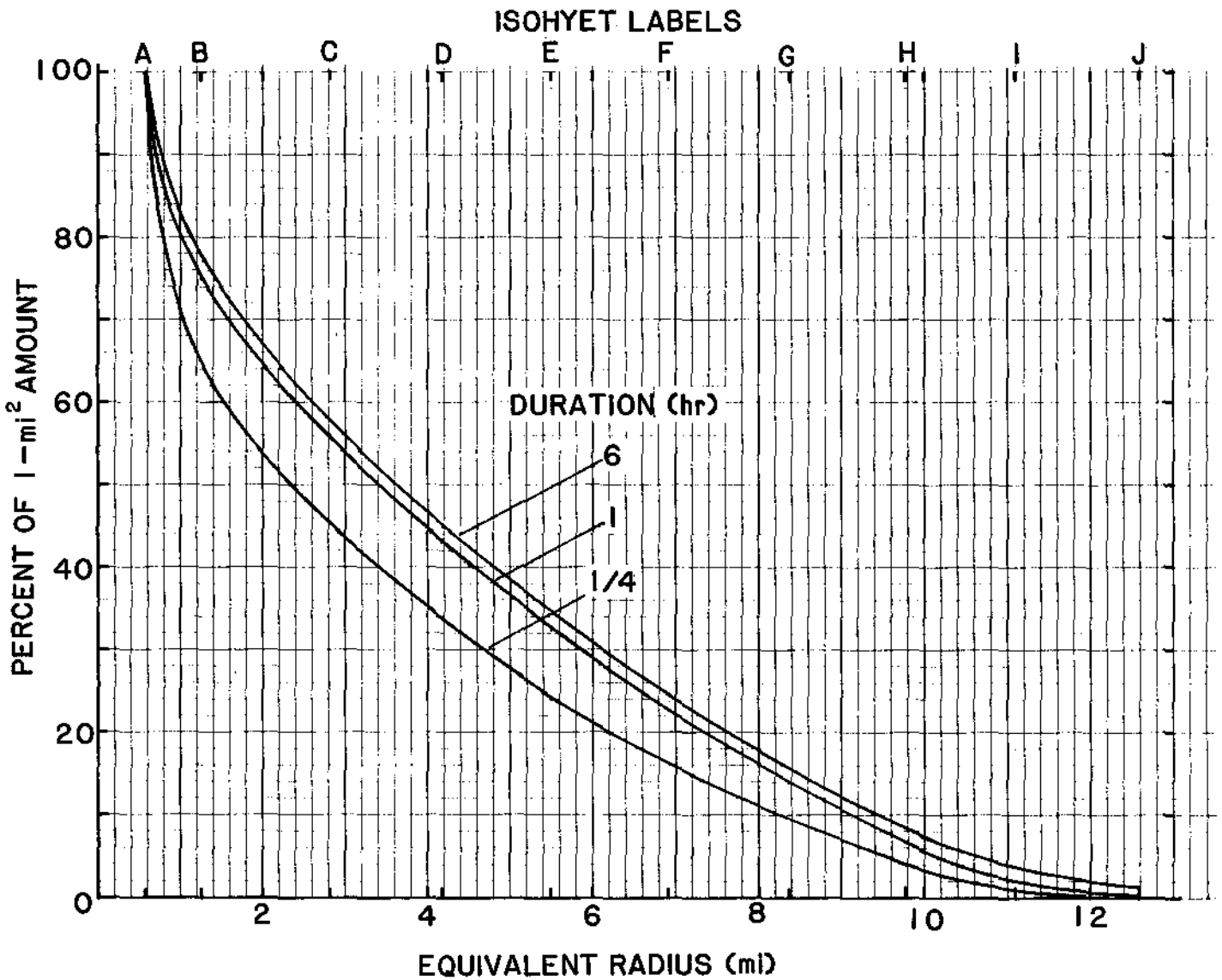

Figure 11.17.--Isohyet profile curves

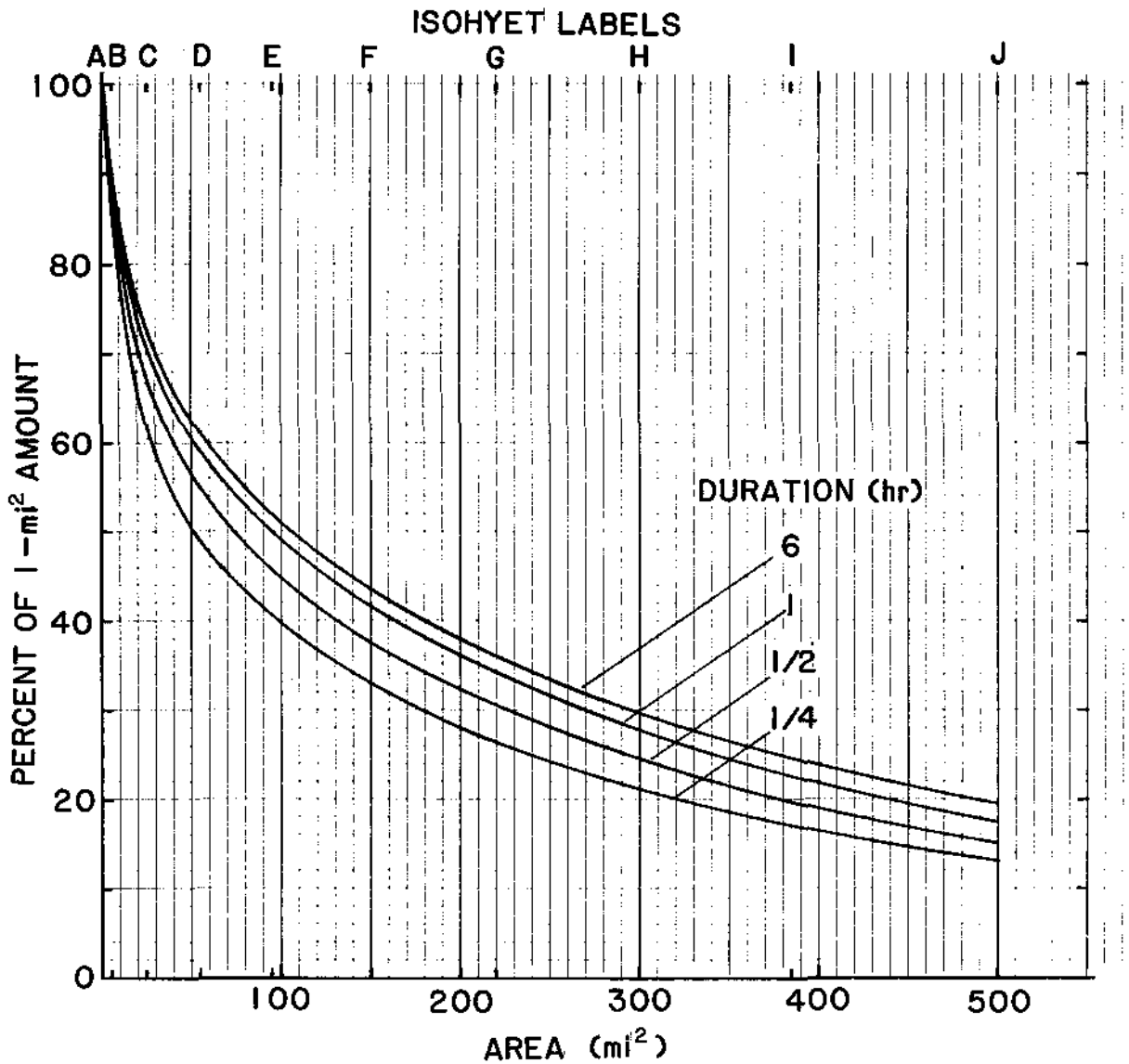

Figure 11.18.--Depth-area relations for HMR 57.

Table 11.10--Depth-Area curves (percent of 1-mi² amount).									
	Duration (hours)								
Isohyet	1/4	1/2	3/4	1	2	3	4	5	6
A	100.0	100.0	100.0	100.0	100.0	100.0	100.0	100.0	100.0
B	85.6	88.6	89.8	89.9	90.4	90.6	90.7	90.7	90.8
C	60.3	66.6	69.1	70.3	71.3	71.8	72.0	72.1	72.2
D	48.7	54.6	57.5	59.0	60.0	60.4	60.6	60.8	60.9
E	40.4	45.7	48.7	50.0	51.0	51.3	51.5	51.7	51.9
F	32.7	37.6	40.4	41.6	42.6	42.9	43.0	43.3	43.5
G	26.3	30.5	33.0	34.2	35.0	35.2	35.4	35.7	36.0
H	21.2	24.5	26.7	27.8	28.6	28.9	29.1	29.4	29.7
I	17.0	19.7	21.6	22.5	23.4	23.6	23.8	24.2	24.5
J	13.2	15.3	16.8	17.5	18.3	18.6	18.9	19.2	19.6

From Table 11.9, the procedure can be worked through for each duration to obtain the corresponding depth-area curves as plotted in Figure 11.18. The results from this effort should be converted to percentages of 100 percent (percent of A-isohyet or 1-mi²) as shown. The results obtained from this process are summarized in the Table 11.10, and are the depth-area curves for this example.

11.9 One-Hour, 1-mi² Local Storm PMP Map

11.9.1 Introduction

An index map of 1-hour, 1-mi² local storm PMP for elevations up to and including 6,000 feet is provided in this study (Figure 11.19). The map was provided for this range of elevations because our research indicated that local storm PMP does not vary appreciably from sea level to this elevation. This approach is consistent with the procedure of previous PMP studies of the western United States (Hansen et al., 1977; Hansen et al., 1988) in which index maps of local storm PMP were provided through 5,000 feet.

11.9.2 Development of 1-hour, 1-mi² Local Storm PMP Map

The greatest moisture maximized 1-hour local storms from Table 11.1 were transposed according to the procedures described in Sections 11.5 and 11.6. For storms in which the most significant precipitation occurred within a period other than 1 hour, the observed precipitation amount was adjusted to an equivalent 1-hour amount using the depth-duration relationship shown in Figure 11.12 or

Table 11.4. The transposed amounts were subsequently merged as closely as possible with the 1-hour, 1-mi^2 5,000-feet local storm PMP amounts for the region east of the Continental Divide (Hansen et al., 1988) and the Southwest (Hansen et al., 1977). Section 11.9.4 describes some of the variations among these studies and the reasons for them.

PMP in the central portion of the study area was controlled by the Morgan, Utah, storm of August 16, 1958, and the Girds Creek, Oregon, storm of July 13, 1956. PMP along the coastal areas was controlled by the Aberdeen 20 NNE, Washington, storm of May 28, 1982. PMP in the western Cascades and the Rockies was implicitly determined from these same storms with the Skykomish 1 ENE, Washington, (May 25, 1945) storm supporting the PMP values in the Cascades, and the Opal, Wyoming, (August 16, 1990) storm supporting the PMP values in the Rockies.

11.9.3 Analysis of Local Storm PMP Map

The highest values of local storm PMP are found over the extreme southeastern portions of the region in the Snake River basin, where a maximum near 10 inches reaches nearly to the Idaho border. It is assumed that the high moisture needed to support a local PMP-type event enters this area during southwest monsoon conditions from the Gulf of California and subtropical southeastern Pacific waters, or secondarily from the Gulf of Mexico (Hansen, 1975).

A broad maximum of 8.0 to 9.0 inches in local storm PMP is evident through the Snake River basin along the western Idaho border with a concomitant dip found over the Rockies. This occurs, despite the fact that persisting dew points are as high and thunderstorm activity is generally more common in the Rockies than in the plateau region. The causes of this may be attributable to two major reasons. First, there are lower daytime temperatures in the summer, July highs at elevations below 4,000 feet average from the low to mid 80's in the Rockies, whereas they range from the mid 80's to low 90's throughout the plateau. The lower surface temperatures engender a more stable atmosphere, which is less conducive to the development of strong convection. Second, the rough terrain of the mountains acts as a barrier for the supply of low-level moisture needed in a PMP-type storm. Although there may be some enhancement of convection due to forced lifting of the air by the mountainous terrain, it does not appear that this is enough to offset moisture limitations at higher elevations. It is recognized that the Rockies are the most data sparse area in the study region and that very heavy local rains may have been altogether missed. Future studies using paleo-flood analysis may be helpful here.

Local storm PMP values decrease generally to the north and west across the region, falling to near 6.0 inches in the Cascades east of Seattle. This is in response to both decreased moisture and the diminished intensity of solar radiation. Monsoonal and subtropical Pacific moisture has difficulty in penetrating the numerous obstacles to northward penetration as reflected in the maximum persisting dew-point maps.

The minimum in local storm PMP, about 3.0 inches, occurs along the outer tip of the Olympic Peninsula in Washington. This value increases to a little over 5.0 inches southward along the coast, at the Oregon-California border. These relatively low values are due to the stabilizing effect of the cool, moist layer of surface air that results from interaction with the cool Pacific ocean waters along the coast. Conversely, the warm, unstable air masses that produce heavy local thunderstorms over the plateau region are obstructed from westward movement by the Cascade range. Heavy local storms in the coastal areas also seem to occur under considerably different meteorological conditions than those in the interior.

11.9.4 Comparison with Other Studies

HMR 43 calculated summer thunderstorm PMP for areas of the Columbia River basin east of the Cascades. The procedures used in that study vary significantly from those utilized in the current study and are discussed at various points throughout this publication. A brief review of the salient differences in procedures and results will serve to emphasize the types of changes involved.

Figure 11.20 shows a difference map between HMR 57 and HMR 43 for 1-hour, 1-mi^2 PMP in inches east of the Cascades. The majority of the region falls within a one-half inch departure between the two studies. Slightly larger differences however, appear in the study area from about central Washington to the Canadian border. The new study results in PMP from 1 to 1.5 inches lower (negative values).

Comparisons were also made with adjoining studies, including HMR 49 and HMR 55A. Some of the different assumptions regarding elevation and durational characteristics have already been discussed.

Relative to HMR 49, the differences in 1-hour, 1-mi^2 PMP are near zero in extreme northern Utah, becoming more positive (i.e., the new values are higher) moving westward to a maximum of about +1.5 inches along the California-Oregon border area. The primary reason for this discrepancy may come from transposing the Morgan, Utah, storm throughout the southern portions of the Northwest. HMR 49 and the present study support a preferred seasonality of storms and do not attempt to apply seasonal curves or nomograms.

No significant PMP differences exist in local storm PMP between the current study and HMR 55A. No major new storms were found within this general area which would cause any increase in PMP to be made, and no evidence was revealed which might indicate a lowered estimate. Seasonality for HMR 55A showed a distinct summer maxima in extreme local storms, a finding in agreement with this study as well.

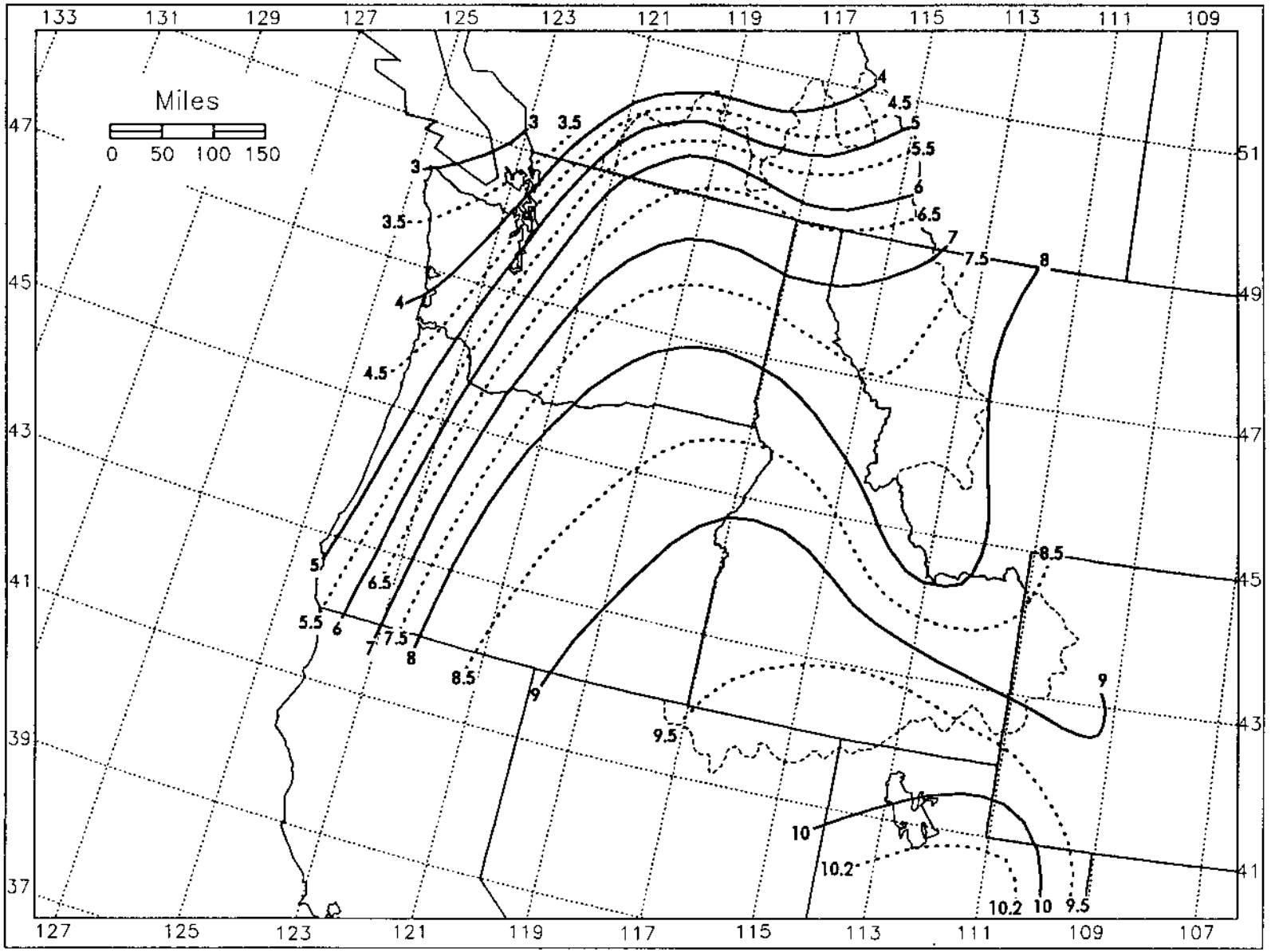

Figure 11.19.--1-hour, 1-mi² local storm PMP in inches for elevations to 6000 feet.

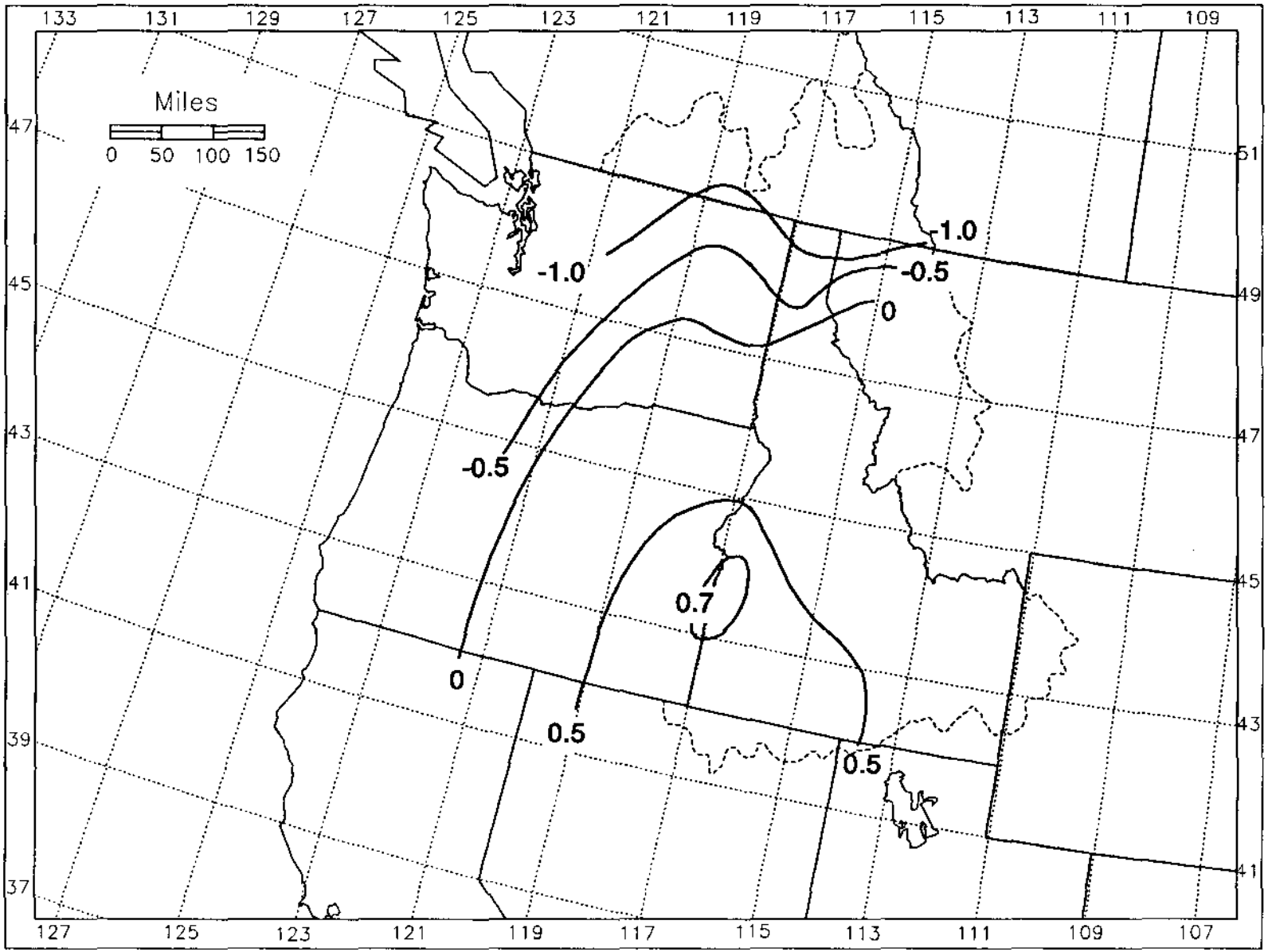

Figure 11.20.--Map of differences between 1-hour, 1-mi^2 PMP amounts from HMR 57 and HMR 43.

12. INDIVIDUAL DRAINAGE PMP COMPARISONS

Early in the development of criteria to redefine PMP for the northwest United States, it was recognized by the various participants and potential users of this information that comparisons between individual drainage PMP estimates, previously defined in HMR 43 and those derived from the present study, would be extremely useful. Significant differences noted would serve as a critical test bed for justification of the new data and methodologies employed. Additionally, where significant differences existed, such locations were noted as those having a major impact on both existing as well as immediately planned water control projects in the surrounding region.

Of the participating federal agencies, both COE and Reclamation were in the best position to select individual drainages for evaluation. A total of 47 individual drainages were assembled (32 Reclamation and 15 COE). Figure 12.1 portrays the general location of the selected drainages. Circled numbers represent COE basins, and dots represent Reclamation basins. The actual location of the dam site may be somewhat removed from the basin centroids shown in Figure 12.1. The selection of representative drainages was not only decided upon by immediate planning needs of the various agencies, but was based on providing a diverse array of test locations over the entire region. Judicious selection enhanced the evaluation of the level of PMP due to variations in terrain features such as elevation, exposure and drainage area size.

PMP (HMR 43 and as revised in this study) was calculated for both general and local storms (where applicable) for each of the 47 drainages. In order to reasonably control the number of possible computations, certain limits were applied to the evaluation. General storm PMP was computed only for the months of June and December and for durations of 1, 6, 24, 48, and 72 hours. In accordance with criteria from HMR 43, general storm 1-hour PMP was not evaluated for drainages greater than 200-mi^2 in area size. Local storm PMP was evaluated for the month of greatest potential (HMR 43), or as in the present study, only an all-season[1] local storm PMP value was determined. In accord with criteria stated in HMR 43, local storm PMP was not provided for drainages located west of the Cascade Mountain Divide. For both PMP studies (HMR 43 and present), local storm PMP was limited to those drainages comprising a total basin area of approximately 500-mi^2 or less. Additionally, only the 1- and 6-hour local storm PMP were evaluated.

Within the criteria described above, Table 12.1 provides a comparison of PMP for selected drainages as determined from procedures followed in this report and those from HMR 43, respectively. For the general storm comparison, months of June and December and durations of 1, 6, 24, 48, 72 hours, the change in PMP

---

[1]All-season - Greatest PMP that could happen sometime during the year.

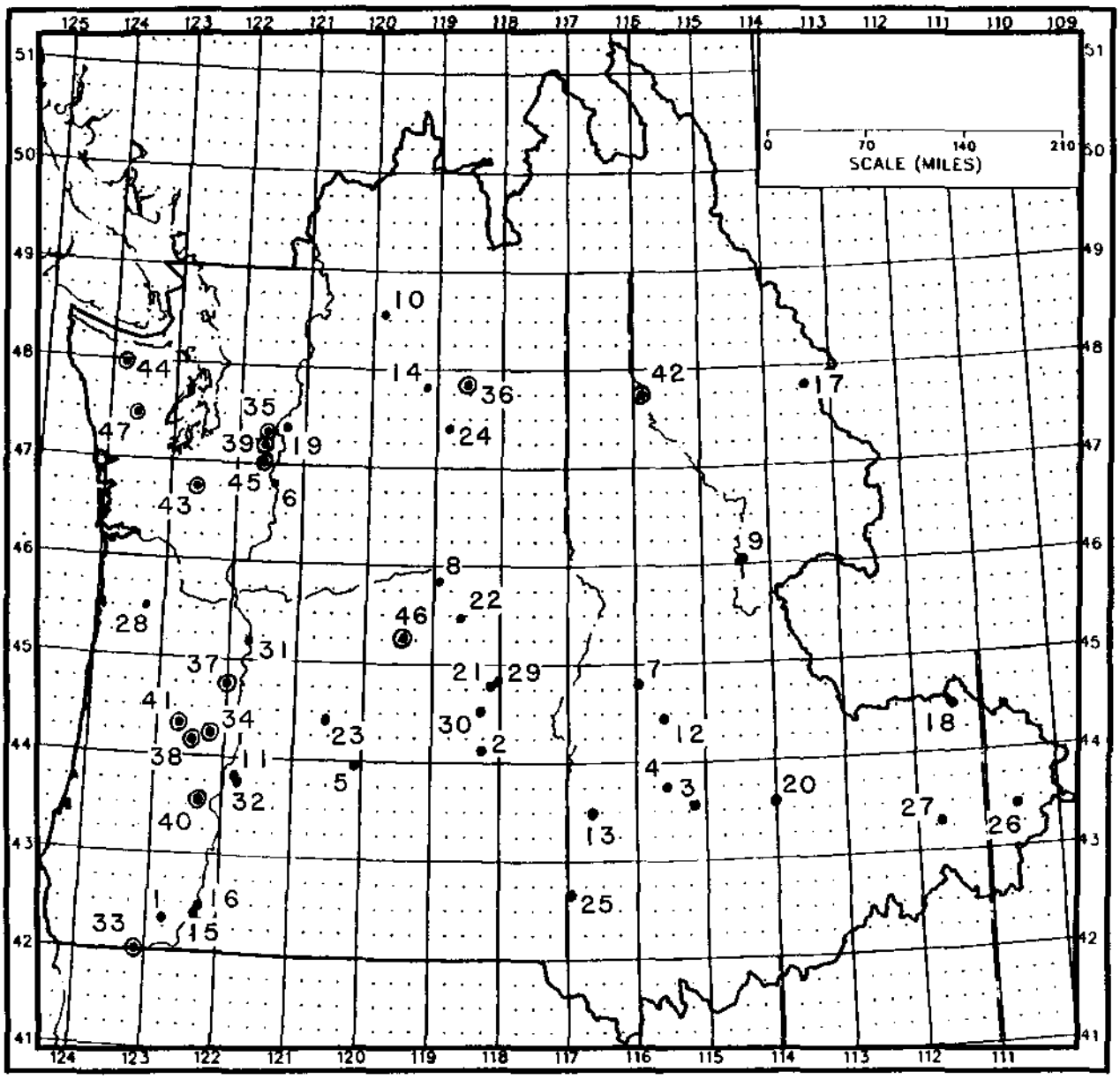

Figure 12.1.--Test basin location map. Index numbers refer to basins listed in Table 12.1. Dots are centroids of Reclamation basins and circled dots are centroids of COE basins.

ranges from a plus 98 percent (revised PMP greater than HMR 43) to a minus 63 percent (revised PMP less than HMR 43). The mean change for all 47 basins examined was minus 8 percent, indicating a moderate overall reduction in general storm PMP from that computed using HMR 43. Table 12.2 provides an overall comparison (for June and December and for 1-72 hours) of the percentage changes in general storm PMP between values computed for this study versus those values determined from HMR 43.

Similarly, changes in local storm PMP (results also shown in Table 12.1) resulted in a range of plus 12 to minus 28 percent for the 1-hour duration. The mean change in 1-hour PMP resulted in a slight reduction, minus 3 percent of local storm PMP over the study region. For 6 hours, the range varied between a minus 24 to a minus 53 percent. At 6 hours, the mean change in PMP was significantly reduced, to a minus 40 percent.

In addition to the determination of PMP from both the present and previous studies, initial estimates of PMP were converted into flood hydrographs from which peak and volume flood flows were determined. These results were not relevant to the present study, but may be obtained from Reclamation.